



Search for exotic decays of the Higgs boson to a pair of pseudoscalars in the $\mu\mu b\bar{b}$ and $\tau\tau b\bar{b}$ final states

CMS Collaboration*

CERN, 1211 Geneva 23, Switzerland

Received: 20 February 2024 / Accepted: 25 March 2024
© CERN for the benefit of the CMS Collaboration 2024

Abstract A search for exotic decays of the Higgs boson (H) with a mass of 125 GeV to a pair of light pseudoscalars a_1 is performed in final states where one pseudoscalar decays to two b quarks and the other to a pair of muons or τ leptons. A data sample of proton–proton collisions at $\sqrt{s} = 13$ TeV corresponding to an integrated luminosity of 138 fb^{-1} recorded with the CMS detector is analyzed. No statistically significant excess is observed over the standard model backgrounds. Upper limits are set at 95% confidence level (CL) on the Higgs boson branching fraction to $\mu\mu b\bar{b}$ and to $\tau\tau b\bar{b}$, via a pair of a_1 s. The limits depend on the pseudoscalar mass m_{a_1} and are observed to be in the range $(0.17\text{--}3.3) \times 10^{-4}$ and $(1.7\text{--}7.7) \times 10^{-2}$ in the $\mu\mu b\bar{b}$ and $\tau\tau b\bar{b}$ final states, respectively. In the framework of models with two Higgs doublets and a complex scalar singlet (2HDM+S), the results of the two final states are combined to determine upper limits on the branching fraction $\mathcal{B}(H \rightarrow a_1 a_1 \rightarrow \ell\ell b\bar{b})$ at 95% CL, with ℓ being a muon or a τ lepton. For different types of 2HDM+S, upper bounds on the branching fraction $\mathcal{B}(H \rightarrow a_1 a_1)$ are extracted from the combination of the two channels. In most of the Type II 2HDM+S parameter space, $\mathcal{B}(H \rightarrow a_1 a_1)$ values above 0.23 are excluded at 95% CL for m_{a_1} values between 15 and 60 GeV.

1 Introduction

The discovery of the Higgs boson (H) by the ATLAS and CMS experiments at the CERN LHC [1–3] strengthened the case for the standard model (SM), which states that the electroweak (EW) symmetry is broken by a complex scalar field [4–9]. However, the SM is not a complete theory as it cannot account for a number of experimental observations. For example, the origin of neutrino mass and dark matter remains unexplained in the SM. Several beyond the SM (BSM) theories address these observations while identifying the 125 GeV resonance as part of an extended group of scalar

particles. The Two-Higgs-Doublet Models (2HDMs) [10–12] predict five physical scalar and pseudoscalar particles and allow different couplings of each scalar to SM fermions. The two real scalar singlet extension [13,14] of the SM results in three neutral scalar bosons. A broad class of 2HDMs extended with an additional complex scalar singlet (2HDM+S) contains seven physical scalar and pseudoscalar particles [11]. In all these models, one of the scalars is identified as the discovered Higgs boson with a mass of 125 GeV.

Recent measurements of the Higgs boson’s couplings at the LHC do not rule out exotic decays of the Higgs boson to BSM particles. The ATLAS and CMS experiments put, respectively, 12 and 16% upper bounds on the branching fraction of the Higgs boson to undetected particles at 95% confidence level (CL) using data collected in 2016–2018 (Run 2) [15,16]. Given these bounds, it is crucial to examine the data for direct evidence of new particles coupling to the Higgs boson, in particular, to test possible extensions of the SM.

The exotic decay channels may include the Higgs boson decaying to a pair of light pseudoscalar particles that subsequently decay to pairs of SM particles. This signal can be experimentally discriminated from SM Higgs boson decays. These decays arise naturally in the phenomenology of 2HDM+S, which is described here in more detail. The 2HDM+S couplings are such that a fermion can couple to only one of the scalar doublets to avoid flavor changing neutral currents at tree level. Under this condition, four types of 2HDM+S models are possible [11,17]. While the SM-like couplings of the Higgs boson to fermions and gauge bosons can be preserved, the singlet state of the 2HDM+S can also serve as a dark matter candidate that couples to the Higgs boson [18,19]. In 2HDM+S scenarios of Type I, the second doublet, ϕ_2 , can couple to any fermion whereas the first doublet, ϕ_1 , cannot couple to fermions. In Type II models, ϕ_1 couples to down-type quarks and charged leptons while ϕ_2 couples to up-type quarks. This model is close to the next-to-minimal supersymmetric SM (NMSSM), which is a special case of 2HDM+S and provides a solution to the so-

* e-mail: cms-publication-committee-chair@cern.ch (corresponding author)

called μ -problem [20,21]. The NMSSM particle spectrum contains two pseudoscalars, a_1 and a_2 , the lighter a_1 can have a mass smaller than the Higgs boson to allow $H \rightarrow a_1 a_1$ decays. Another valid extension has quarks coupling to ϕ_2 and charged leptons coupling to ϕ_1 , referred to as the Type III or “lepton-specific” model. Finally, in the Type IV or “flipped” model, ϕ_2 couples to up-type quarks and charged leptons while ϕ_1 couples to down-type quarks [11,17].

The branching fraction, \mathcal{B} , of $a_1 a_1 \rightarrow \text{SM particles}$ depends on the type of 2HDM+S model, the mass of the pseudoscalar, m_{a_1} , and the ratio of the vacuum expectation values of the two doublets, $\tan \beta$. The decay width of a_1 to fermion pairs depends, in addition, on the mass of the decay products. In Type II 2HDM+S models, $\mathcal{B}(a_1 a_1 \rightarrow \tau \tau b \bar{b})$ is slightly above 10%, while it can reach up to $\sim 50\%$ in Type III models. The large predicted branching fraction makes this channel particularly attractive. The decay of a_1 pairs to $\mu \mu b \bar{b}$ has a much smaller branching fraction. In Type III models, for $\tan \beta = 2$, $\mathcal{B}(a_1 a_1 \rightarrow \mu \mu b \bar{b})$ is predicted to be about 0.2%. Despite the small branching fraction, this channel can provide competitive results given the high performance of the muon reconstruction and the excellent dimuon mass resolution in CMS. The possibility of the Higgs boson decaying into a pair of a_1 s is studied in this paper for both $\tau \tau b \bar{b}$ and $\mu \mu b \bar{b}$ decay modes. The gluon-gluon fusion production mechanism (ggF) constitutes the dominant Higgs bosons production process, with a cross section of $\sigma_{\text{ggF}}^{13\text{TeV}} = 48.58 \pm 1.56 \text{ pb}$ [22] at next-to-next-to-next-to-leading order ($N^3\text{LO}$) accuracy in perturbative quantum chromodynamics (QCD) and next-to-leading order (NLO) in EW corrections. The contribution of the Higgs boson production through vector boson fusion (VBF) is also taken into account with a cross section of $\sigma_{\text{qqH}}^{13\text{TeV}} = 3.72 \pm 0.08 \text{ pb}$ [22], which includes NLO QCD and EW corrections.

Similar searches have been performed at the LHC. The latest analysis by the ATLAS Collaboration [23] has placed a strong bound of $\mathcal{B}(H \rightarrow a_1 a_1 \rightarrow \mu \mu b \bar{b}) < (0.2\text{--}4) \times 10^{-4}$ in the range $16 < m_{a_1} < 62 \text{ GeV}$, using the LHC Run 2 data at $\sqrt{s} = 13 \text{ TeV}$, extending its prior analysis with a partial data sample [24]. The existing CMS search at this center-of-mass energy [25] is based on a data sample corresponding to an integrated luminosity of 36 fb^{-1} and results in an upper limit on $\mathcal{B}(H \rightarrow a_1 a_1 \rightarrow \mu \mu b \bar{b})$ of $(1\text{--}7) \times 10^{-4}$, considering m_{a_1} between 20 and 62.5 GeV. At 8 TeV, the CMS experiment has provided an upper bound of $\mathcal{B}(H \rightarrow a_1 a_1 \rightarrow \mu \mu b \bar{b}) < (2\text{--}8) \times 10^{-4}$ [26]. In the $\tau \tau b \bar{b}$ final state, an upper limit of $\mathcal{B}(H \rightarrow a_1 a_1 \rightarrow \tau \tau b \bar{b}) < (3\text{--}12) \times 10^{-2}$ was reported by CMS using a 36 fb^{-1} dataset at $\sqrt{s} = 13 \text{ TeV}$, where m_{a_1} ranged between 15 and 60 GeV [27]. The analysis examined both leptonically and hadronically decaying τ leptons, the latter denoted by τ_h .

This paper reports an extension of CMS searches [25,27] with the proton–proton (pp) collision data collected in Run 2, corresponding to an integrated luminosity of 138 fb^{-1} at 13 TeV. Improved techniques in these analyses bring higher sensitivity to the allowed branching fractions. In the $\mu \mu b \bar{b}$ final state, in particular, a more in-depth study of the signal achieves a greater gain in sensitivity than that offered by the additional LHC data alone. This channel looks for a bump over the dimuon mass spectrum after a cut-based event selection. A neural network approach to optimize the signal region (SR) selection provides better sensitivity to the signal processes in the $\tau \tau b \bar{b}$ channel. The results in the two final states are combined, and interpretations are provided in different types of 2HDM+S models.

The paper is organized as follows: Sects. 2 and 3 discuss the CMS detector and the simulated data samples used in these analyses. The event reconstruction and event selection procedures are presented in Sects. 4 and 5, respectively. The background prediction methods are described in Sect. 6. Section 7 presents the signal extraction methods, and the discussion of the systematic uncertainties can be found in Sect. 8. Results and interpretations are detailed in Sect. 9 and a summary is presented in Sect. 10. Tabulated results of this analysis are provided in the HEPData record [28].

2 The CMS experiment

The central feature of the CMS apparatus is a superconducting solenoid of 6 m internal diameter, providing a magnetic field of 3.8 T. Within the solenoid volume are a silicon pixel and strip tracker, a lead tungstate crystal electromagnetic calorimeter (ECAL), and a brass and scintillator hadron calorimeter (HCAL), each composed of a barrel and two endcap sections. Forward calorimeters extend the pseudorapidity (η) coverage provided by the barrel and endcap detectors. Muons are detected in gas-ionization chambers embedded in the steel flux-return yoke outside the solenoid. The collision data are recorded with the help of Level-1 (L1) trigger, high-level trigger (HLT), and data acquisition systems ensuring high efficiency in selecting interesting physics events [29]. A more detailed description of the CMS detector, along with a definition of the coordinate system used and the relevant kinematic variables, can be found in Ref. [30].

3 Simulated event samples

Simulated samples are used to design and optimize the analysis strategy and, where needed, to estimate background contributions. A number of Monte Carlo (MC) event generators are used to produce events using either leading order (LO) or NLO matrix element calculations. In all cases, parton

showering and fragmentation are implemented using PYTHIA (version 8.212) [31]. The description of parton distribution functions (PDFs) relies on the NNPDF3.1 set [32]. Jets produced at the matrix element level are matched with those generated by PYTHIA using the MLM [33, 34] method for LO samples. The FxFx matching [35] is implemented in the case of NLO samples generated with MADGRAPH5_aMC@NLO (version 2.2.2 for the simulation of the 2016 data and 2.4.2 for 2017–2018) [36]. For the underlying event description, the CUETP8M1 [37] tune was used for MC samples simulating the 2016 data, while for those simulating the 2017–2018 data, the CP5 [38] tune was employed. The GEANT4 [39, 40] package has been used for the detector simulation. To model the effect of additional collisions within the same or adjacent bunch crossings (pileup), minimum bias interactions are simulated and superimposed on the hard-scattering events. Simulated events are then reweighted to reproduce the pileup distribution in data.

The $H \rightarrow a_1 a_1 \rightarrow \mu\mu b\bar{b}$ signal events are generated with the NMSSMHET model [17] using MADGRAPH5_aMC@NLO (version 2.6.5) at LO [34]. Both ggF and VBF Higgs boson production mechanisms are considered, within the a_1 mass range of 15–60 GeV. While the ggF samples are generated with 5 GeV steps in m_{a_1} , the VBF samples are generated only for m_{a_1} of 20, 40, and 60 GeV. Interpolation methods are used to estimate the signal yield and the shape of the dimuon resonance for all mass hypotheses. Similar settings are used to produce $H \rightarrow a_1 a_1 \rightarrow \tau\tau b\bar{b}$ signal events at 11 a_1 masses between 12 and 60 GeV, for both ggF and VBF Higgs boson production modes.

The major backgrounds for the analyses are the Drell–Yan (DY) process ($Z/\gamma^* + \text{jets}$), the production of a top quark–antiquark pair with additional jets (denoted tt+jets), single top quark production, and massive vector boson pair production (Diboson). In the $\mu\mu b\bar{b}$ channel, the background estimation is performed using methods fully based on control samples in data with no reference to simulation. Simulated background samples are, however, used to optimize the signal selection criteria. In the $\tau\tau b\bar{b}$ channel, only the backgrounds from DY production with $Z \rightarrow \tau\tau$, QCD multijet events in the $e\mu$ final state, and events with jets misidentified as τ_h candidates are estimated using control samples in data.

The DY process in the dilepton final state is modeled using MADGRAPH5_aMC@NLO. Based on the dilepton invariant mass ($m_{\ell\ell}$) threshold at the generator level, two DY samples are considered, one with $m_{\ell\ell} > 50$ GeV and the other with $10 < m_{\ell\ell} < 50$ GeV. The high-mass DY samples are produced at (N)LO, with up to four (two) additional partons at the matrix element level. For the low mass, samples are primarily produced at LO with additional partons, similar to those of high mass, while NLO and LO samples inclusive in number of jets are also utilized. In the $\mu\mu b\bar{b}$ analysis, the NLO samples at high mass are employed, and at low mass,

NLO QCD K-factors are applied to the LO cross section. An uncertainty of 30% is considered on these K-factor corrections, as they are extracted from NLO low-mass samples with limited number of events. The accuracy of the DY sample is found to be sufficient for optimization purposes, which is the only use of the simulated backgrounds in the $\mu\mu b\bar{b}$ channel. The $\tau\tau b\bar{b}$ analysis makes use of LO DY samples in the entire mass range. The cross sections are normalized to next-to-NLO (NNLO) in QCD using K-factors [41]. In addition, the Z boson p_T distribution is corrected by reweighting simulated events to data in bins of $m_{\ell\ell}$ and the p_T of the dilepton system.

The POWHEG BOX v2.0 framework [42–45] event generator is used to produce tt+jets and single top events at NLO. The simulated tt+jets events are reweighted to match the top quark p_T distribution at NNLO QCD and NLO EW [46] precision. Diboson and W+jets events are generated by MADGRAPH5_aMC@NLO. Similar to the high-mass DY sample, W+jets events are simulated with up to four additional partons at the matrix element level for all years. The tt+jets, DY, and W+jets samples are normalized to cross section values accurate to NNLO in QCD [47–55]. All SM backgrounds containing the Higgs boson are generated using POWHEG v2.0 at NLO [56–60].

4 Object reconstruction

The $\mu\mu b\bar{b}$ and $\tau\tau b\bar{b}$ analyses together reconstruct a diverse set of final-state particles for a $H \rightarrow a_1 a_1$ signal. The $\mu\mu b\bar{b}$ analysis relies on the presence of two prompt muons. In the $\tau\tau b\bar{b}$ channel, on the other hand, final states with at least one τ lepton decaying to an electron or muon, i.e., $e\mu$, $e\tau_h$, and $\mu\tau_h$, are considered. The τ lepton decays resulting in same-flavor leptons, or in two τ_h candidates, are not included as they bring negligible sensitivity to the analysis. The signal acceptance of $\tau_h\tau_h$ is very low due to high trigger thresholds, whereas ee and $\mu\mu$ final states suffer from low branching fractions.

The particle-flow (PF) algorithm [61] is used to reconstruct and identify each individual particle (PF candidate) in the event, with an optimized combination of information from the various elements of the CMS detector. The energy of photons is measured in ECAL. The energy of electrons is determined from a combination of the electron momentum at the primary interaction vertex as measured by the tracker, the energy of the corresponding ECAL cluster, and the energy sum of all bremsstrahlung photons spatially compatible with originating from the electron track. The energy of muons is obtained from the curvature of the corresponding track. The energy of charged hadrons is evaluated via a combination of their momentum measured in the tracker and the matching of the ECAL and HCAL energy deposits, corrected for the response function of the calorimeters to hadronic showers.

Finally, the energy of neutral hadrons is obtained from the corresponding corrected ECAL and HCAL energies.

The primary vertex (PV) is taken to be the vertex corresponding to the hardest scattering in the event, identified using the tracking information alone, as described in Section 9.4.1 of Ref. [62].

Muons can be produced directly in a_1 decays in the $\mu\mu b\bar{b}$ final state, or from decays of the τ leptons in the $\tau b\bar{b}$ channel. In both analyses, muons must lie within $|\eta| < 2.4$. The p_T threshold for muons in the $\tau b\bar{b}$ analysis depends on the trigger selection, see Sect. 5 and Table 1. In the $\mu\tau_h$ final state, it is required to be 1 GeV greater than the HLT muon p_T threshold in order to be in a region where the efficiency of the respective trigger is independent of p_T . The muon p_T requirement in the $e\mu$ final state, selected with an $e\mu$ trigger, is 24(13) GeV when the muon is the leading (subleading) lepton in the pair. In the $\mu\mu b\bar{b}$ analysis, the leading (subleading) muon p_T must exceed 17 (15) GeV. The two muons are required to have an opposite electric charge and to be separated by a minimum $\Delta R \equiv \sqrt{(\Delta\eta)^2 + (\Delta\phi)^2} = 0.4$, where ϕ is the azimuthal angle of the particle's momentum in the plane perpendicular to the beam line. In cases where more than two muons satisfy these criteria, the pair with the highest p_T are considered.

In order to suppress contributions from nonprompt decays of hadrons and from their shower penetration in the muon detectors, selected muons must pass dedicated identification requirements. The so-called tight identification [63] is used in the $\mu\mu b\bar{b}$ analysis with an efficiency varying between 95 and 99%, depending on η , where the data and simulation agree within 1–3%. Looser requirements for muons, known as medium identification criteria [63], are employed in the $\tau b\bar{b}$ analysis, with an overall efficiency of 99.5% for simulated W and Z events.

The lepton isolation variable I_{rel} is calculated by summing the transverse energy deposited by other particles in a cone of size $\Delta R = 0.4(0.3)$ around the muon (electron) and dividing by the lepton p_T . The contribution of charged particles from pileup is suppressed by requiring the charged particles to be associated with the PV. An average pileup energy is subtracted from the total energy of neutral particles and photons within the isolation cone, since vertex association is not known in this case. Muons are required to pass $I_{\text{rel}} < 0.15$ in the $\tau b\bar{b}$ analysis.

In the $\mu\mu b\bar{b}$ analysis, a looser requirement of $I_{\text{rel}} < 0.25$ is imposed, which results in about 99% efficiency for muons with $p_T > 20$ GeV, independent of η [63]. Electrons from τ lepton decays are selected within $|\eta| < 2.4$ with different p_T thresholds, according to the $\tau b\bar{b}$ final state. In the $e\mu$ channel, the threshold is 24 GeV if the electron is the leading lepton. Otherwise, it is reduced to 13 GeV. In the $e\tau_h$ channel, the electron p_T must be more than 1 GeV beyond the HLT threshold. A multivariate analysis (MVA) discriminant

is used to identify electrons. The MVA exploits several properties of the electron candidate, including energy deposits in the ECAL, the quality of the associated track, and the shower shape in the calorimeters [64]. The chosen MVA working point has a 90% efficiency to correctly identify an electron. Identified electrons are further required to be isolated, fulfilling $I_{\text{rel}} < 0.10$. In the $e\mu$ channel of the $\tau b\bar{b}$ analysis, the electron must be separated from the muon by $\Delta R \geq 0.3$ and have an opposite electric charge. For both electrons and muons, correction factors for the reconstruction and identification efficiencies are obtained from data and applied to simulation.

Jets are reconstructed by clustering the charged and neutral PF candidates using the anti- k_T algorithm [65,66] with a distance parameter of 0.4, up to $|\eta| < 4.7$ for tagging VBF events. The reconstructed jet energy is corrected for effects from the detector response as a function of the jet p_T and η . Furthermore, contamination from pileup and electronic noise is subtracted using the charged-hadron subtraction method [61]. To achieve a better agreement between data and simulation, an extra η -dependent smearing is performed on the jet energy in simulated events [67,68]. Events are required to have at least two (one) jets with $|\eta| < 2.4$ and $p_T > 15$ (20) GeV in the $\mu\mu b\bar{b}$ ($\tau b\bar{b}$) analysis. Jets are required to be separated from any selected electron, muon, or τ_h by $\Delta R > 0.4$ (0.5) in the $\mu\mu b\bar{b}$ ($\tau b\bar{b}$) analysis.

Both channels rely on identifying jets that likely originate from b quarks. The DEEPIET flavor classification algorithm [69,70] is used to tag b jets. Three different working points on the b tagging discriminator values correspond to 0.1, 1, and 10% misidentification probabilities, known respectively as tight (T), medium (M), and loose (L) working points. The misidentification probability to tag a light-flavour jet as a b jet is measured in inclusive QCD multijet MC samples, and they depend on the p_T and η of the jet. The corresponding b tagging efficiencies, measured in tt+jets events, are about 65, 80, and 95%, respectively [71]. In the $\mu\mu b\bar{b}$ analysis, the selected jet with the higher b tagging score is required to pass the tight working point whereas the second one fulfills the loose b tagging requirements. In this paper the latter is referred to as the ‘looser’ b jet. In the $\tau b\bar{b}$ analysis, the medium working point is used to identify b jets. The shape of the distribution of the b tagging discriminator, and thus the b tagging efficiencies, can be different between data and simulation. Since the $\mu\mu b\bar{b}$ analysis relies on the b tagging discriminator distribution, shape-based corrections are applied on simulation to match the data. A similar method is used in the $\tau b\bar{b}$ final state, which, by construction corrects the b tagging efficiency for all b tagging discriminator scores.

The hadron-plus-strips algorithm [72] with anti- k_T jets as seeds is used to reconstruct the hadronically decaying τ leptons. The algorithm combines one or three tracks with energy deposits in the calorimeters to identify the τ lepton

Table 1 The electron, muon, and τ_h p_T thresholds in GeV at trigger level for the $\mu\mu bb$ and $\tau\tau bb$ channels

Year	Single/dilepton trigger p_T	$\mu\mu bb$ μ	$\tau\tau bb$					
			$e\mu$ e μ		$e\tau_h$ e τ_h		$\mu\tau_h$ μ τ_h	
2016	Single lepton	24	–	–	25	–	22	–
	p_T -leading lepton	17	23	23	–	–	–	20
	p_T -subleading lepton	8	12	8	–	–	19	–
2017	Single lepton	24	–	–	27, 32	–	24, 27	–
	p_T -leading lepton	17	23	23	–	30	–	27
	p_T -subleading lepton	8	12	8	24	–	20	–
2018	Single lepton	24	–	–	32, 35	–	24, 27	–
	p_T -leading lepton	17	23	23	–	30	–	27
	p_T -subleading lepton	8	12	8	24	–	20	–

decay modes. Neutral pions are reconstructed as strips with a dynamic size in η - ϕ from reconstructed electrons and photons, where the strip size varies as a function of the p_T s of the electron or photon candidate. The p_T of the τ_h candidates are required to be 5 GeV greater than the threshold at the trigger level. In events triggered by single leptons, the τ_h p_T must exceed 20 GeV. The pseudorapidity of the τ_h candidate also depends on the trigger. It is restricted to $|\eta| < 2.1$ if a τ_h identification is performed at the HLT, and to $|\eta| < 2.3$ otherwise. To distinguish genuine τ_h decays from electrons, muons, or jets originating from the hadronization of quarks or gluons, the DEEPTAU algorithm [73] is used. Information from all individual reconstructed particles near the τ_h candidate axis is combined with properties of the τ_h candidate. The probability for a jet to be misidentified as a τ_h candidate by the DEEPTAU algorithm depends on the p_T and the jet flavor. In simulated W+jets events, the misidentification rate for jets is estimated to be 0.4% for a genuine τ_h identification efficiency of 70%. The misidentification rate for electrons (muons) is 2.6% (0.03%) for a genuine τ_h identification efficiency of 80% (> 99%). In the $e\tau_h$ and $\mu\tau_h$ final states of the $\tau\tau bb$ channel, the τ_h candidate must be separated from the electron or muon by $\Delta R \geq 0.4$ and they must be oppositely charged.

The missing transverse momentum vector \vec{p}_T^{miss} is computed as the negative vector sum of the transverse momenta of all the PF candidates in an event, and its magnitude is denoted as p_T^{miss} [74]. The \vec{p}_T^{miss} is modified to account for corrections to the energy scale of the reconstructed jets in the event. Anomalous high- p_T^{miss} events can be due to a variety of reconstruction failures, detector malfunctions or noncollision backgrounds. Such events are rejected by event filters that are designed to identify more than 85–90% of the spurious high- p_T^{miss} events with a mistagging rate less than 0.1% [74].

5 Event selection

Table 1 summarizes the different p_T criteria for online reconstructed electrons, muons and τ_h s in the $\mu\mu bb$ and $\tau\tau bb$ channels.

The $\mu\mu bb$ event candidates are selected based on the requirement that either one or both muons are reconstructed at the HLT. Passing the double-muon trigger necessitates two isolated muons with p_T exceeding thresholds of 17 and 8 GeV, which increases to 24 GeV for an isolated muon in the single-muon trigger path. Accepting events from both single- and double-muon triggers improves the trigger efficiency by including events in which the second muon is not reconstructed at the trigger level.

Depending on the decay of the τ lepton and the data-taking period, the $\tau\tau bb$ candidates must pass either a single-electron, single-muon, $e\mu$, $e\tau_h$, or $\mu\tau_h$ trigger selection. The single-muon, $e\mu$ and $\mu\tau_h$ triggers require the reconstructed muon to be isolated, while electron isolation is required for the single-electron, $e\mu$ and $e\tau_h$ triggers. Two $e\mu$ dilepton triggers have been used for all data-taking years, having p_T thresholds of 23 (23) and 12 (8) GeV for the p_T -leading and -subleading lepton of the trigger in the case of electrons (muons). The single-muon and single-electron triggers with p_T thresholds of 22 and 25 GeV, respectively, are used for analyzing the 2016 data. The p_T thresholds of electron and τ_h candidates are, respectively, 24 and 30 GeV for the $e\tau_h$ dilepton trigger in the 2017–2018 data. For the $\mu\tau_h$ dilepton trigger, the p_T thresholds of muon and τ_h are, respectively, 19 (20) and 20 (27) GeV for the data taken during 2016 (2017–2018). The increase in the p_T threshold is necessary to control the trigger rate at a larger instantaneous luminosity. Similarly, the p_T requirements are tightened for single-lepton triggers across the years. This results in two different thresholds for single-electron and muon triggers for 2017–2018.

Offline, in the $\mu\mu bb$ channel events are required to have two muons and at least two b jets passing the kinematic, iden-

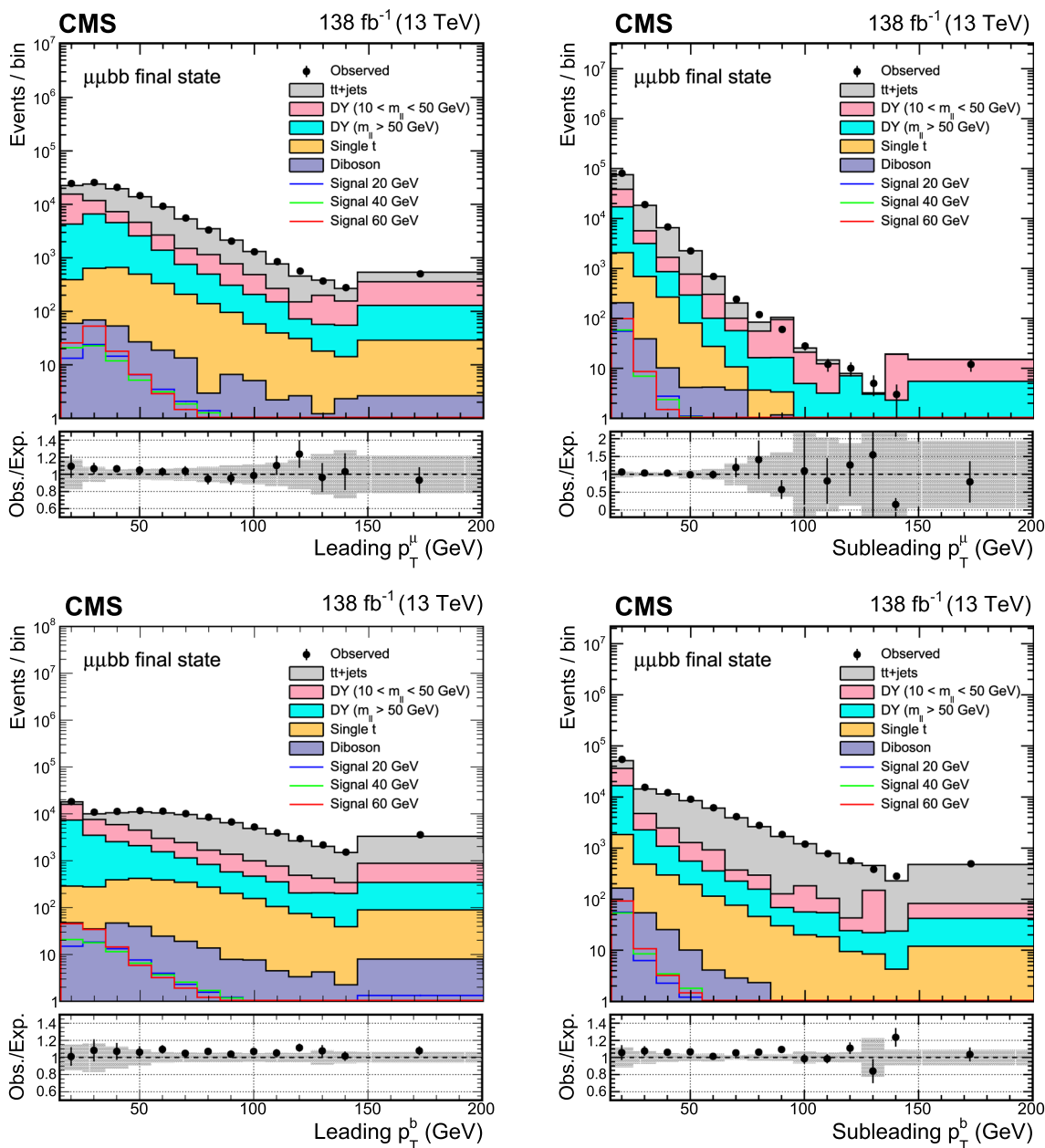


Fig. 1 The distributions of leading and subleading (upper) muon p_T and (lower) b jet p_T in the selected events. The uncertainty band in the lower panel represents the limited size of the simulated samples together with a 30% uncertainty in the low-mass DY cross section. Simulated

samples are normalized using the corresponding theoretical cross sections. To evaluate the normalization of the signal, SM Higgs boson cross sections are multiplied by the $\mathcal{B}(a_1 a_1 \rightarrow \mu \mu b b)$ value that is calculated in the Type III model with $\tan \beta = 2$

tification, and isolation criteria detailed in Sect. 4. While the final search in this channel is performed for m_{a_1} between 15 and 62.5 GeV, events are selected with a dimuon invariant mass, $m_{\mu\mu}$, between 14 and 70 GeV. The additional sidebands in $m_{\mu\mu}$ help model the backgrounds at the boundaries. To reduce the background contribution from tt+jets, events with $p_T^{\text{miss}} > 60$ GeV are rejected. The selection yields a total of 109 821 data events while the corresponding expected

yield from simulated backgrounds is $103\,900 \pm 7300$. The background contribution should be compared with about 80–100 expected signal events, depending on m_{a_1} , from both ggF and VBF Higgs boson production. The branching fraction $\mathcal{B}(a_1 a_1 \rightarrow \mu \mu b b)$ is evaluated in the Type III model with $\tan \beta = 2$. Figure 1 shows, in data and simulation, the p_T distributions of the p_T -leading and -subleading muons and b jets. Although the estimation of backgrounds in this

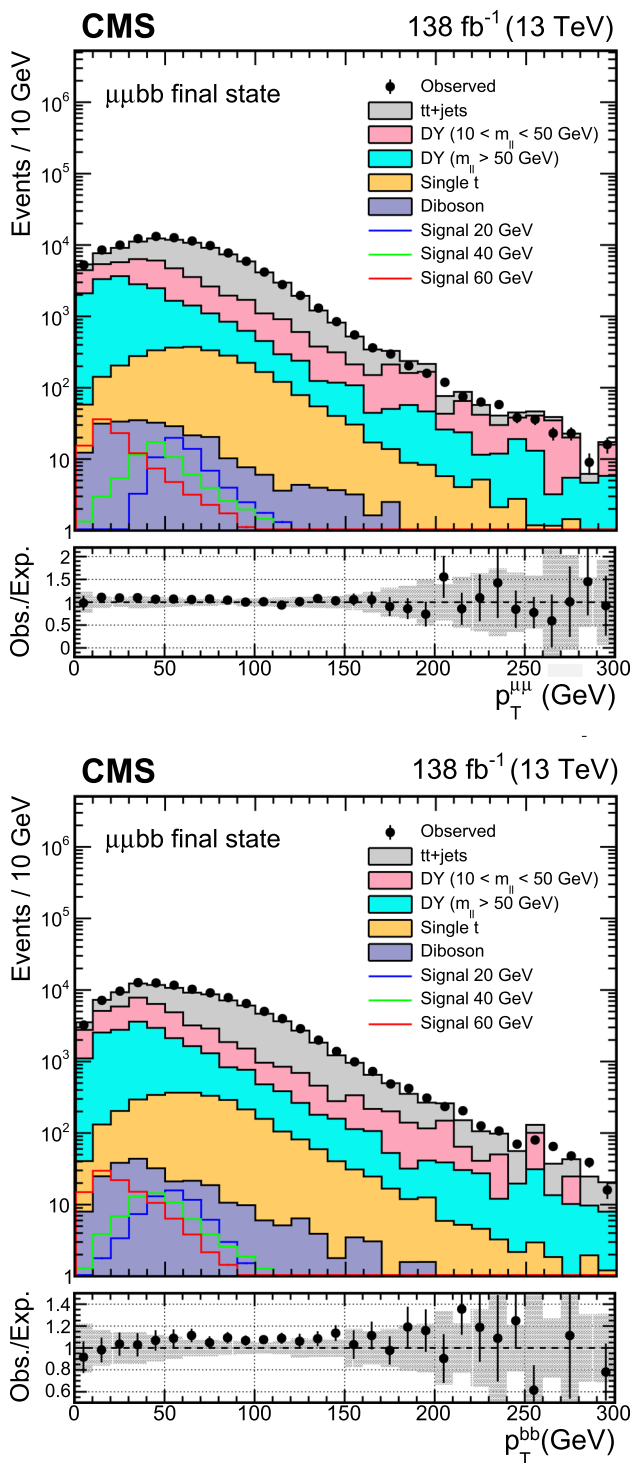


Fig. 2 The p_T distributions of the (upper) dimuon systems and (lower) di-b-jet system. The uncertainty band in the lower panel represents the limited size of the simulated samples together with a 30% uncertainty in the low-mass DY cross section. Simulated samples are normalized to using the corresponding theoretical cross sections. To evaluate the normalization of the signal, SM Higgs boson cross sections are multiplied by the $B(a_{1A_1} \rightarrow \mu\mu bb)$ value that is calculated in the Type III model with $\tan \beta = 2$

analysis does not rely on simulation, the observed level of agreement between data and simulation justifies the use of simulated events to optimize the sensitivity. Figure 2 shows distributions for the p_T of the dimuon ($p_T^{\mu\mu}$) and the di-b-jet systems (p_T^{bb}).

To further suppress backgrounds, a χ_{tot}^2 variable is defined as $\chi_{tot}^2 = \chi_{bb}^2 + \chi_H^2$. It examines the compatibility of $m_{\mu\mu}$ and m_{bb} with m_{a_1} , and of $m_{\mu\mu bb}$ with the Higgs boson mass in signal events. The components of χ_{tot}^2 are defined as

$$\chi_{bb} = \frac{(m_{bb} - m_{\mu\mu})}{\sigma_{bb}} \quad \text{and} \quad \chi_H = \frac{(m_{\mu\mu bb} - 125 \text{ GeV})}{\sigma_H}. \quad (1)$$

The variables σ_{bb} and σ_H are the mass resolutions of the di-b-jet system and the Higgs boson candidate, respectively, which are derived from Gaussian fits to simulated distributions of m_{bb} and the mass of the Higgs boson candidate. While σ_H is found to be constant, σ_{bb} increases linearly with m_{a_1} and is modeled as a function of $m_{\mu\mu}$ ($\sigma_{bb} = am_{\mu\mu} + b$), assuming $m_{\mu\mu} = m_{a_1}$. The χ_{tot}^2 variable is evaluated on an event-by-event basis. It was shown in Ref. [25] that applying a threshold on χ_{tot}^2 leads to a large suppression of backgrounds while keeping the majority of signal events. Such a requirement translates to a circle centered at zero in the 2D-plane of χ_{bb} and χ_H , as shown in Fig. 3. However, the χ_{bb} and χ_H components are clearly correlated as can be seen in Fig. 3 (lower). This leads to a loss of signal efficiency when imposing the circular requirement. In addition, both χ_{bb} and χ_H distributions are slightly biased away from zero, adding more inefficiencies. Therefore, in the current analysis the definitions of the variables were adjusted to be unbiased and uncorrelated.

The correlation between the χ_{tot} components, as well as their bias, depends on m_{a_1} . The bias is modeled as a function of $m_{\mu\mu}$ and is corrected event by event. After applying this correction, a principal component analysis [75] is performed on the bias-corrected variables. The bias-corrected variables are therefore transformed using the eigenvalues, λ_1 and λ_2 , and eigenvectors $\begin{pmatrix} a \\ b \end{pmatrix}$, of the correlation matrix:

$$\begin{pmatrix} \chi_H \\ \chi_{bb} \end{pmatrix}_d = \begin{pmatrix} \frac{a}{\sqrt{\lambda_1}} & \frac{b}{\sqrt{\lambda_1}} \\ -\frac{b}{\sqrt{\lambda_2}} & \frac{a}{\sqrt{\lambda_2}} \end{pmatrix} \begin{pmatrix} \chi_H \\ \chi_{bb} \end{pmatrix}_c, \quad \chi_d^2 \equiv \chi_{H,d}^2 + \chi_{bb,d}^2 \quad (2)$$

with subscripts d and c, respectively, standing for decorrelated and bias-corrected components of χ_{tot} . The transformation matrix in Eq. (2) has three independent parameters, $a/\sqrt{\lambda_1}$, $a/\sqrt{\lambda_2}$, and b/a , that are modeled as functions of m_{a_1} . Figure 4 compares the performance of the selection based on χ_d^2 and χ_{tot}^2 variables in terms of the signal ($m_{a_1} = 40 \text{ GeV}$) efficiency and background rejection probability. Based on the optimization studies, events with $\chi_d^2 < 1.5$ are selected.

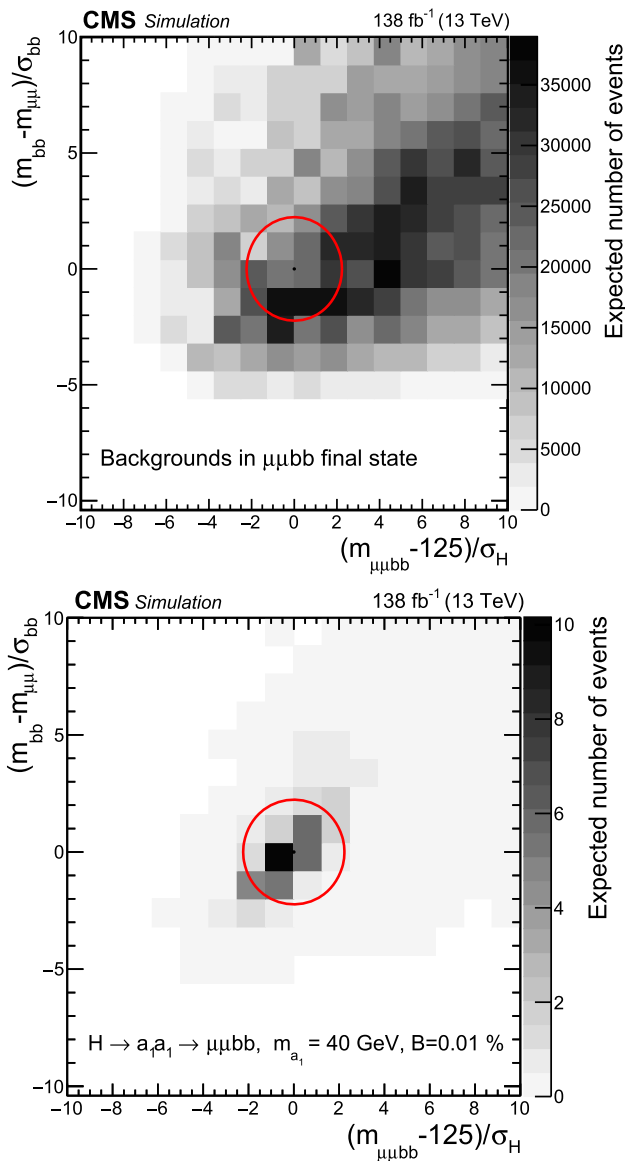


Fig. 3 The distribution of χ_{bb} versus χ_H as defined in Eq. (1) for (upper) simulated background processes and (lower) the signal process with $m_{a_1} = 40$ GeV. The contours indicate lines of constant χ_{tot}^2 . The gray scale represents the expected yields in data. To evaluate the yield of the signal, SM Higgs boson cross sections are multiplied by the $\mathcal{B}(a_1 a_1 \rightarrow \mu\mu bb)$ value that is calculated in the Type III model with $\tan \beta = 2$

Table 2 summarizes the number of observed events in data together with the expected yields for the main backgrounds and the signal for different m_{a_1} hypotheses.

Events are further categorized according to the jet p_T , the b tagging score of the jets, and additional jet activity in the event compatible with the VBF signature. Events containing at least one of the two selected b jets with $p_T < 20$ GeV are put in a separate category (Low p_T). This category brings extra sensitivity to the signals with lower m_{a_1} values and contains about 70% (40%) background (ggF signal) events. For

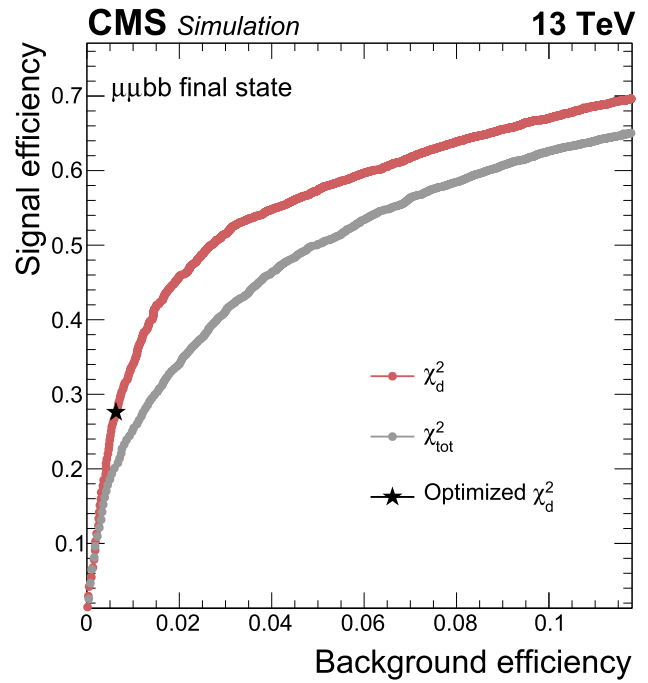


Fig. 4 Signal ($m_{a_1} = 40$ GeV) versus background efficiency for different thresholds on χ_{tot}^2 (gray) and χ_d^2 (red) variables. The black star indicates signal efficiency versus that of background for the optimized χ_d^2 requirement

Table 2 Event yields in the $\mu\mu bb$ channel for simulated processes and the number of observed events in data after applying $\chi_d^2 < 1.5$. The expected number of simulated events is normalized to the integrated luminosity of 138 fb^{-1} . The Type III parametrization of 2HDM+S with $\tan \beta = 2$ is used to evaluate $\mathcal{B}(a_1 a_1 \rightarrow \mu\mu bb)$

Process	Yield
tt+jets	86.3 ± 2.2
DY ($10 < m_{\ell\ell} < 50$ GeV)	289.6 ± 89.5
DY ($m_{\ell\ell} > 50$ GeV)	200.2 ± 31.9
Diboson	1.5 ± 0.9
Single top	11.4 ± 1.6
Total expected background	589.1 ± 95.1
Data	641

Signal for ggH ($\mu\mu bb$)		
$m_{a_1} = 20$ GeV	$m_{a_1} = 40$ GeV	$m_{a_1} = 60$ GeV
15.4 ± 0.2	18.7 ± 0.2	40.5 ± 0.3

the VBF category, events must have at least two jets, in addition to b jets, with $p_T > 30$ GeV, $|\eta| < 4.7$, and an invariant mass $m_{jj} > 250$ GeV. About 50% of VBF signal events fall in this category. The remaining events are categorized based on the b tagging score of the looser b jet. Three exclusive categories are defined where the second jet passes the loose but fails the medium (TL), passes the medium but fails the tight (TM), and passes the tight (TT) b tagging working point. This

Table 3 Summary of the categorization requirements in the $\mu\mu b\bar{b}$ channel. Events in these categories contain two muons and two b jets. As stated in the text, L, M, and T stand for the loose, medium, and tight b tagging criteria, respectively

Categories for selected events	
Low p_T	At least one b jet with $p_T < 20$ GeV
VBF	Two additional jets with $p_T > 30$ GeV, $ \eta < 4.7$, and $m_{jj} > 250$ GeV
TL	Looser b jet passes L but fails M
TM	Looser b jet passes M but fails T
TT	Looser b jet passes T

categorization relies on the fact that events with genuine and misidentified b quark jets are distributed differently among those categories. About 20% of backgrounds as well as the ggF signal events fall into the TL category. The TM and TT categories almost equally receive 20% of the ggF signal and 5% of the background events. Table 3 summarizes the categories of the current analysis, whereas the expected yields in different categories are presented in Table 4.

In the $\tau\tau b\bar{b}$ channel, the offline signal event signature constitutes at least one b jet, and depending on the τ lepton decay mode, an $e\mu$, an $e\tau_h$, or a $\mu\tau_h$ pair. Any event with an additional electron or muon is rejected to reduce the contribution from DY and multilepton processes. The selection and identification requirements for all objects are discussed in Sect. 4.

Each final state is subdivided into two categories based on the presence of exactly one b jet or at least two b jets in the event. Requiring at least two b jets in the event introduces an additional category compared to Ref. [27], capable of reconstructing the full signal hypothesis and bringing further signal-to-background discrimination power. In total there are six event categories, considering the number of b jets and the decay modes of the τ leptons. A deep neural network (DNN) with two hidden layers and 40 nodes is used to discriminate signal from background events in each category. The DNNs are trained using simulated events.

Kinematic properties of the decay products are utilized to construct variables that are inputs to the DNN training,

such as the p_T and transverse mass (m_T) of the leptons and b jets, p_T and η of the di- τ system, the invariant mass of each system made of a lepton and a b jet, and ΔR between various combinations of the identified particles. One of the most important discriminating observables used in the training is the invariant mass of the decay products of the τ leptons and the p_T -leading b jet, denoted by $m_{b\tau\tau}$. The $m_{b\tau\tau}$ value is typically smaller for signal than for background events. Similarly, angular separation and other invariant mass variables can be reconstructed with different combinations of the four final-state particles, employing the correlation between the resonance decay products. The m_T between an e or μ and p_T^{miss} is one of the discriminating variables and is defined as

$$m_T(e/\mu, p_T^{\text{miss}}) \equiv \sqrt{2p_T^{e/\mu} p_T^{\text{miss}} [1 - \cos(\Delta\phi)]}, \tag{3}$$

where $p_T^{e/\mu}$ is the transverse momentum of the lepton and $\Delta\phi$ is the azimuthal angle between the lepton direction and \vec{p}_T^{miss} . Events from tt+jets and misidentified τ_h backgrounds, such as W+jets, have larger p_T^{miss} , thus result in higher m_T values.

Another variable useful in the training is D_ζ , defined as

$$D_\zeta \equiv p_\zeta - 0.85 p_\zeta^{\text{vis}}, \tag{4}$$

where the bisector of the directions of the visible τ decay products transverse to the beam direction is denoted as the ζ axis. The quantity p_ζ is defined as the component of the \vec{p}_T^{miss} along the ζ axis, and p_ζ^{vis} to be the sum of the components of the lepton transverse momentum along the same direction [76]. The $Z \rightarrow \tau\tau$ background corresponds to large D_ζ values because the p_T^{miss} is approximately collinear to the $\tau\tau$ system. The tt+jets events tend to have small D_ζ values due to a large p_T^{miss} that is not aligned with the $\tau\tau$ system. The signal has intermediate D_ζ values because the p_T^{miss} is approximately aligned with the $\tau\tau$ system, but its magnitude is small.

For events in the category with two or more b jets, a variable can be constructed to measure the difference between the invariant mass of the two b jets and the invariant mass of the $\tau\tau$ system ($m_{\tau\tau}$):

$$\Delta m_{a_1} \equiv (m_{b\bar{b}} - m_{\tau\tau})/m_{\tau\tau}. \tag{5}$$

Table 4 The expected yields for backgrounds and different signal hypotheses in each category of the $\mu\mu b\bar{b}$ channel

Category	Signal for ggH ($\mu\mu b\bar{b}$)			Expected background
	$m_{a_1} = 20$ GeV	$m_{a_1} = 40$ GeV	$m_{a_1} = 60$ GeV	
Low p_T	7.4 ± 0.1	7.3 ± 0.1	17 ± 0.2	421 ± 88
VBF	$0.2 \pm (< 0.1)$	$1.0 \pm (< 0.1)$	1.1 ± 0.4	5 ± 2
TL	2.1 ± 0.1	2.8 ± 0.1	6.7 ± 0.1	109 ± 30
TM	2.7 ± 0.1	3.3 ± 0.1	7.7 ± 0.1	27 ± 15
TT	2.8 ± 0.1	4.2 ± 0.1	8.1 ± 0.1	28 ± 11
Total	15.4 ± 0.2	18.7 ± 0.2	40.5 ± 0.3	589 ± 95

This variable is of particular interest since it peaks at zero for signal events. The $m_{\tau\tau}$ distribution reconstructed with the SVfit algorithm [77] is used to test the presence of signal, and thus is not directly included as an input to the DNN.

Figure 5 shows, as an example, the DNN score distributions in the $\mu\tau_h$ channel separated for events with one or at least two b jets. The distributions are obtained by comparing the estimated signal and background distributions of the DNN score to that of the data before the fit described in Sect. 7 (pre-fit).

In each category, subregions are defined using a threshold on the DNN score. The expected limits are scanned by varying the DNN thresholds to obtain the highest sensitivity to the simulated signal. This optimization method also ensures that the expected number of background events in each subregion is large enough to perform the final likelihood fit of the $m_{\tau\tau}$ distribution. There are three SRs for events containing one b jet: SR1, SR2, and SR3, whereas events with two b jets are divided into two categories: SR1 and SR2. The only exception is the $e\tau_h$ final state in the two-b-jet category where no significant gain was observed when adding a second signal region. The remaining subregion containing events with the lowest DNN scores is used as a control region (CR) to constrain various background normalizations in the final likelihood fit.

6 Background estimation

The presence of a $\mu\mu bb$ signal is expected to appear as a peak over the $m_{\mu\mu}$ distribution centered at m_{a_1} . The background shape and its normalization in this channel are collectively determined from data with no reference to simulation. Different parameterizations of polynomials are used to model the $m_{\mu\mu}$ distribution in data of every category, separately. For each group of models, a maximum degree of the polynomial, determined through statistical tests, is imposed. This is to ensure that the data are not overfit. Parameters of every selected model vary within their uncertainties in the final fit to extract the signal strength, defined as the ratio of the observed signal rate to that predicted by the SM. The latter uses the discrete profiling method [78–80] where every functional form of the selected background models is treated as a discrete nuisance parameter. Along with the determination of the signal strength, one of the background models, its parameters, and the corresponding normalization are determined by the fit, as described in Sect. 7.

A major background contribution to the $\tau\tau bb$ channel is $Z \rightarrow \tau\tau$, which is estimated from data using an embedding technique [81]. The method is based on the reconstruction of $Z \rightarrow \mu\mu$ events in data where the muons are replaced with simulated τ leptons with the same kinematic properties. In comparison with the simulation of the $Z \rightarrow \tau\tau$ process,

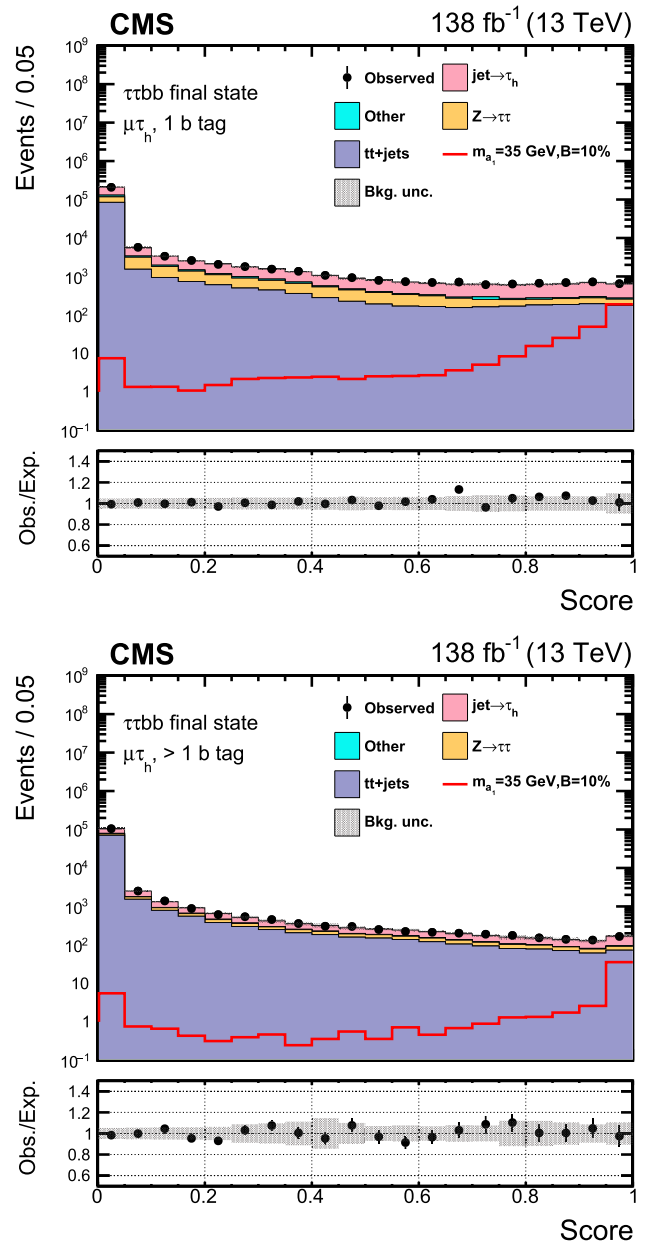


Fig. 5 Pre-fit distributions of the DNN score for the $\mu\tau_h$ channel divided into events with one (upper) or at least two (lower) b jets. The shape of the $H \rightarrow a_1 a_1$ signal, where $m_{a_1} = 35 \text{ GeV}$, is indicated assuming $\mathcal{B}(H \rightarrow a_1 a_1 \rightarrow \tau\tau bb)$ to be 10%. The lower panel shows the ratio of the observed data to the expected yields. The gray band represents the unconstrained statistical and systematic uncertainties

this technique allows a more accurate description of variables related to p_T^{miss} and jet activity. The embedded sample also estimates other SM processes with two genuine τ leptons, such as tt -jets and Diboson.

The QCD multijet contribution to the $e\mu$ final state of the $\tau\tau bb$ channel is estimated using the data in a sideband (SB) region with same-sign $e\mu$ pairs. The event selection in the SB region is otherwise identical to that in the $e\mu$ SRs. The contri-

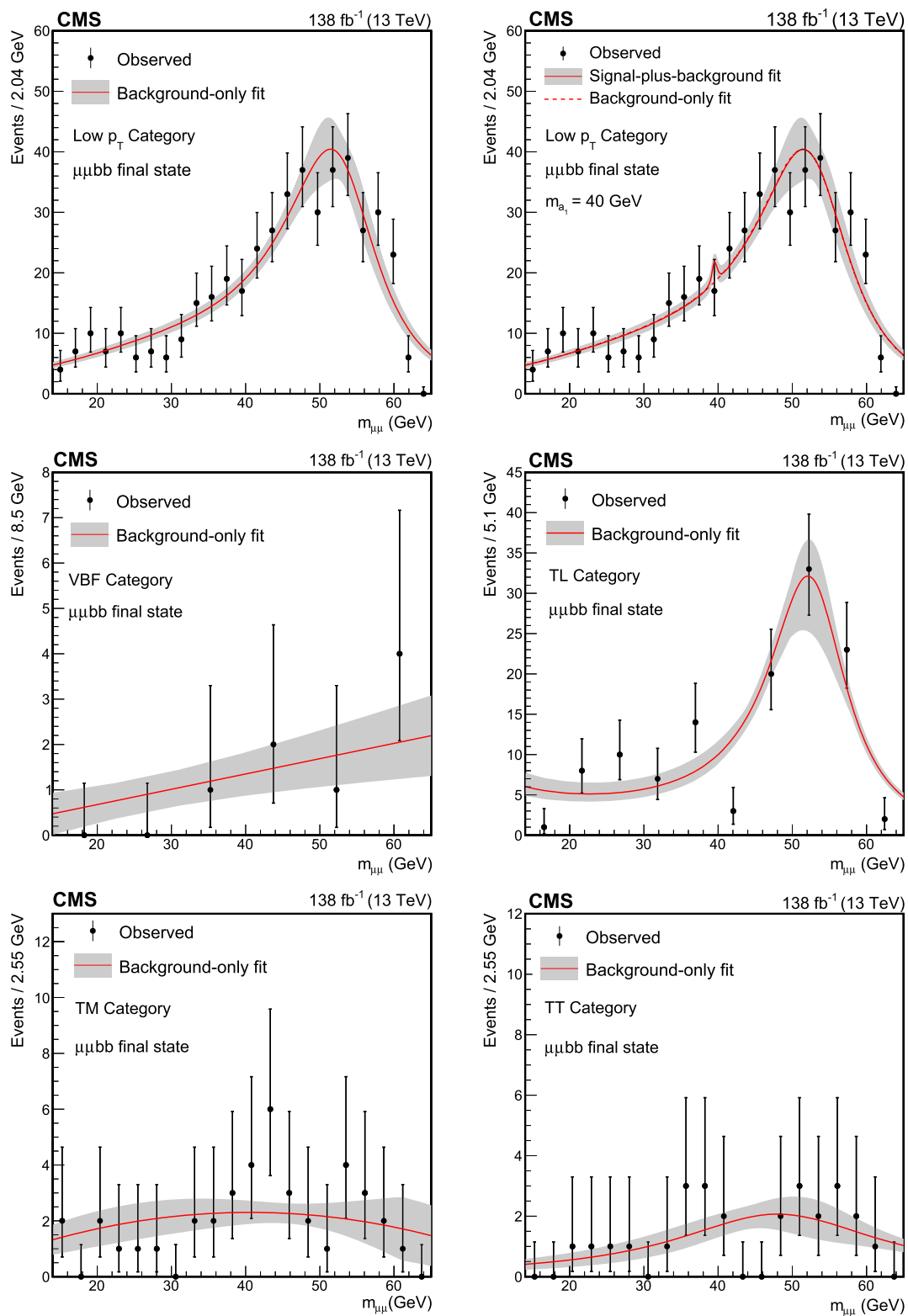


Fig. 6 The best fit background models for the $\mu\mu bb$ channel together with a 68% CL uncertainty band from the fit to the data under the background-only hypothesis for the (upper left) Low p_T category, (middle left) VBF category, (middle right) TL category, (lower left) TM category, and (lower right) TT category.

For comparison, the signal-plus-background is shown for the (upper right) Low p_T category for a signal with $m_{a_1} = 40$ GeV. The expected signal yield is evaluated assuming the SM production of the Higgs boson and $\mathcal{B}(a_1 a_1 \rightarrow \mu\mu bb) = 0.2\%$, as predicted in the Type III 2HDM+S with $\tan \beta = 2$. The bin widths depend on statistics, irrelevant for the final fit

butions of other processes in the SB are taken from simulation and subtracted from the data. The resulting number of data events in the SB is scaled by the ratio of the expected multijet contribution in the SR to the expected multijet contribution in the SB. Scale factors are calculated in data orthogonal to the SR, as functions of the jet multiplicity and the ΔR separation between the electron and the muon, in order to account for possible kinematic differences between the two regions.

Backgrounds with hadronic jets that are misidentified as τ_h candidates contribute significantly to $e\tau_h$ and $\mu\tau_h$ final states and are estimated from data. This background includes the W+jets, QCD multijets, and tt+jets processes with at least one top quark decaying to hadrons. In a data sideband region, events are required to pass all the baseline $e\tau_h/\mu\tau_h$ selection criteria, but fail the τ_h isolation. The data in this SB are reweighted with a factor $f/(1-f)$, where f is the probability for a jet to be misidentified as a τ_h candidate and is evaluated as a function of the $p_T(\tau_h)$. The $Z \rightarrow \mu\mu$ +jets events in data are used to measure the misidentification probability. The final state must contain a dimuon pair compatible with the decay of the Z boson, as well as a τ_h candidate. Simulation is used to subtract from data the contribution from events with a genuine τ_h lepton. The measurement is done separately for the $e\tau_h$ and $\mu\tau_h$ final states. This is because the antilepton discrimination working points in the τ_h identification change depending on the lepton selected is an electron or a muon [73]. The difference between the two fake rate measurements is observed to be around 10%. The misidentification probability also depends on the jet multiplicity, which characterizes the hadronic activity in the event.

Another dominant background is tt+jets, which has to be carefully estimated from simulation. Because tt+jets events with two genuine τ leptons in the final state are an irreducible contribution to the embedded sample described above, the tt+jets background estimate from simulation described here does not include these events. It also does not include tt+jets events in which a reconstructed τ_h candidate arises from a simulated jet, as the estimation of the misidentified τ_h background is derived from data SBs, as described above. The normalization of backgrounds is free to vary within a range limited by the a priori uncertainty estimates in the final fit for the signal extraction.

The presence of a $\tau\tau b\bar{b}$ signal is expected to appear as a peak over the $m_{\tau\tau}$ distribution centered at m_{a_1} . A fit to the $m_{\tau\tau}$ distribution is performed simultaneously in the SRs and CRs described in Sect. 5.

7 Signal extraction

In the $\mu\mu b\bar{b}$ final state, an unbinned maximum likelihood fit to the data $m_{\mu\mu}$ distributions is carried out simultaneously in all event categories. The fit is performed in the range

$15 < m_{\mu\mu} < 62.5$ GeV, using parametric models for signal and background. The parametric model of the signal is a weighted sum of a Voigt profile and a Crystal Ball (CB) function [82], where the mean values of the two are constrained to be identical [25].

Simulated samples are used to determine the parameters of the signal model that may depend on m_{a_1} . The studies are performed separately on signal samples simulated for different years. This is to account for the effect of muon reconstruction details on the signal model in different data-taking periods. Most of the parameters are found to be independent of m_{a_1} and fixed in the final fit. Only the resolutions of the Voigt profile and CB function demonstrate linear variation with the pseudoscalar mass. The slope of the linear models are floating parameters in the signal extraction fit. In each category, contributions from different years are normalized considering the signal selection efficiency and acceptance, and are used to construct the expected signal distribution in data. The expected signal efficiency and acceptance are interpolated for m_{a_1} values not covered by simulation.

To evaluate the background contribution, every selected functional form is treated as a discrete nuisance parameter as discussed earlier. In addition, the parameters of every model, as well as the normalization, are part of the background parameter space. A likelihood \mathcal{L} is constructed using the signal and the background models in all categories, including systematic uncertainties associated with the signal, as nuisance parameters. In the minimization process of the negative logarithm of the likelihood, the discrete profiling method chooses a best fit background model as the physics parameter of interest, the signal strength, varies. The method incorporates the systematic uncertainty in the background model by taking the envelope of the models provided to the fit.

In practice, a penalty term is added to the likelihood to account for the number of free parameters in the final background model. The penalized likelihood, $\tilde{\mathcal{L}}$, is a function of the measured signal strength, μ , the continuous nuisance parameters, $\vec{\theta}$, and the background models, \vec{b} . The penalized likelihood ratio is defined as

$$-2 \ln \frac{\tilde{\mathcal{L}}(\text{data}|\mu, \hat{\theta}_\mu, \hat{b}_\mu)}{\tilde{\mathcal{L}}(\text{data}|\hat{\mu}, \hat{\theta}, \hat{b})}, \quad (6)$$

with the numerator being the maximum $\tilde{\mathcal{L}}$ for a given μ at the best fit values of nuisance parameters and background functions. The denominator is the global maximum of $\tilde{\mathcal{L}}$, obtained at $\mu = \hat{\mu}$, $\theta = \hat{\theta}$, and $b = \hat{b}$. The background function maximizing $\tilde{\mathcal{L}}$ at any μ is used to derive the confidence interval on μ at any m_{a_1} [78]. It is verified that the fit is unbiased using studies where signals at several m_{a_1} values are injected with different strengths. The relative change in signal strength is found to be less than 10^{-4} . The best

fit background models together with their uncertainties are shown in Fig. 6 for all event categories in the $\mu\mu b\bar{b}$ analysis.

In the $\tau b\bar{b}$ channel, a binned maximum likelihood fit is performed on the $m_{\tau\tau}$ distribution with systematic uncertainties included as nuisance parameters. The subregions of event categories from all final states are included in a simultaneous fit. Figures 7, 8 and 9 show the post-fit $m_{\tau\tau}$ distributions in different subregions and categories for the $\mu\tau_h$ final state.

The limits and confidence intervals are obtained using the modified frequentist CL_s approach [83,84] with an asymptotic approximation to the distribution of the profile likelihood ratio test statistic [85]. Pseudoscalar masses between 12 and 60 GeV are considered using simulated samples described in Sect. 3.

The $m_{\mu\mu}$ and $m_{\tau\tau}$ expected distributions are compared to data in a combined fit, integrating over the a_1 decay modes. Integrating over a_1 decays makes the combination model dependent since the branching fraction of a_1 to fermion pairs depends on the model. The 2HDM+S and the theoretical predictions of Ref. [86] are used for the branching fractions of a_1 to muons, τ leptons, and b quarks which are fixed in the fit. The selected events are mutually exclusive in the two analyses as events with an extra muon and/or electron are vetoed in the $\tau b\bar{b}$ selection. A correlation model is employed between the two analyses for the systematic uncertainties that are in common.

8 Systematic uncertainties

The sensitivity of the two analyses, $\mu\mu b\bar{b}$ and $\tau b\bar{b}$, is mainly affected by the uncertainties arising from the finite size of the data sample. Nevertheless, several sources of systematic uncertainties are included in the determination of the results. Most of the systematic uncertainties are common between the two analyses, although their impact on the result may differ. In this class of uncertainties fall those associated with the modeling and acceptance of the signal, including the PDFs, the strong coupling constant, and the renormalization and factorization scales. In addition, experimental uncertainties associated with, e.g., the jet energy calibrations, b tagging, and muon reconstruction and identification are in common between the two analyses, although the uncertainties related to the background estimations are not. In the $\mu\mu b\bar{b}$ analysis, uncertainties associated with the parameters of the dimuon resonance model in the signal are taken into account.

The unbinned maximum likelihood fit of the $\mu\mu b\bar{b}$ analysis accounts for the shape uncertainties in a different way. The impact of systematic variations is found to be negligible on the parametric model of the signal for all m_{a_1} hypotheses. On the other hand, the modeling of the $m_{\mu\mu}$ resolution with m_{a_1} (discussed in Sect. 7) has an uncertainty that is included in the fit with a Gaussian profile. Uncertainties asso-

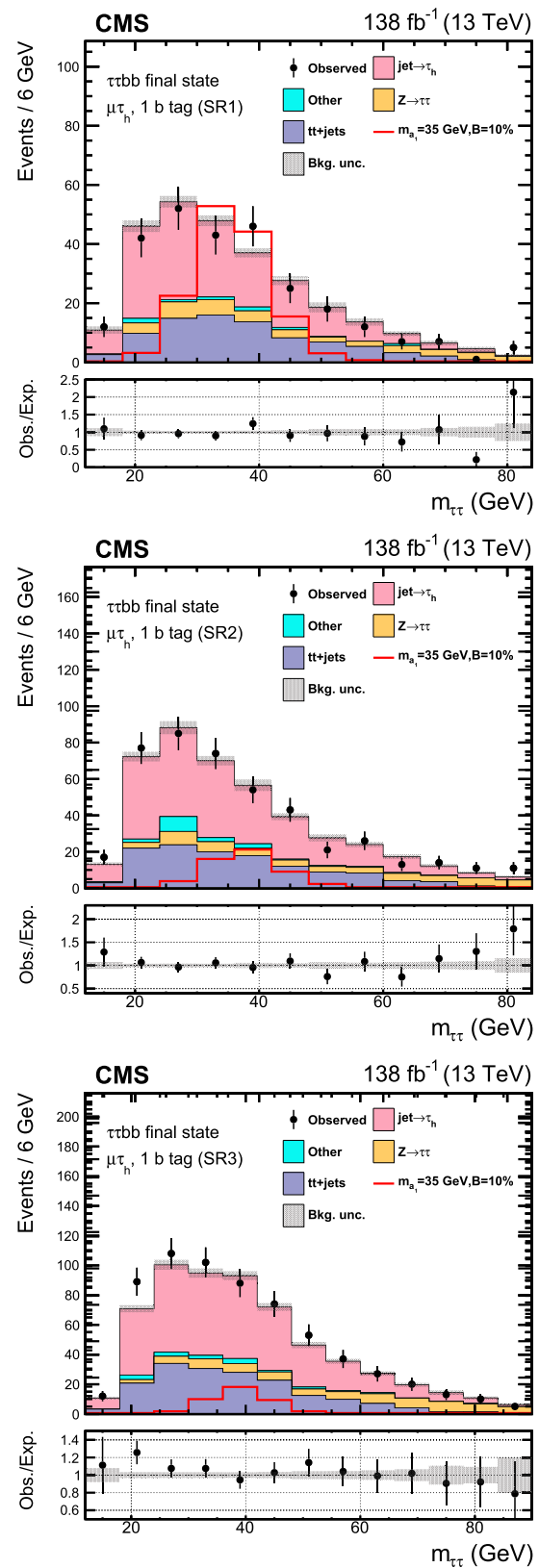


Fig. 7 Post-fit distributions of $m_{\tau\tau}$ for the $\mu\tau_h$ channel signal regions in events with exactly one b tagged jet: SR1 (upper), SR2 (middle), and SR3 (lower). The shape of the $H \rightarrow a_1 a_1$ signal, where $m_{a_1} = 35 \text{ GeV}$, is indicated assuming $B(H \rightarrow a_1 a_1 \rightarrow \tau b\bar{b})$ to be 10%

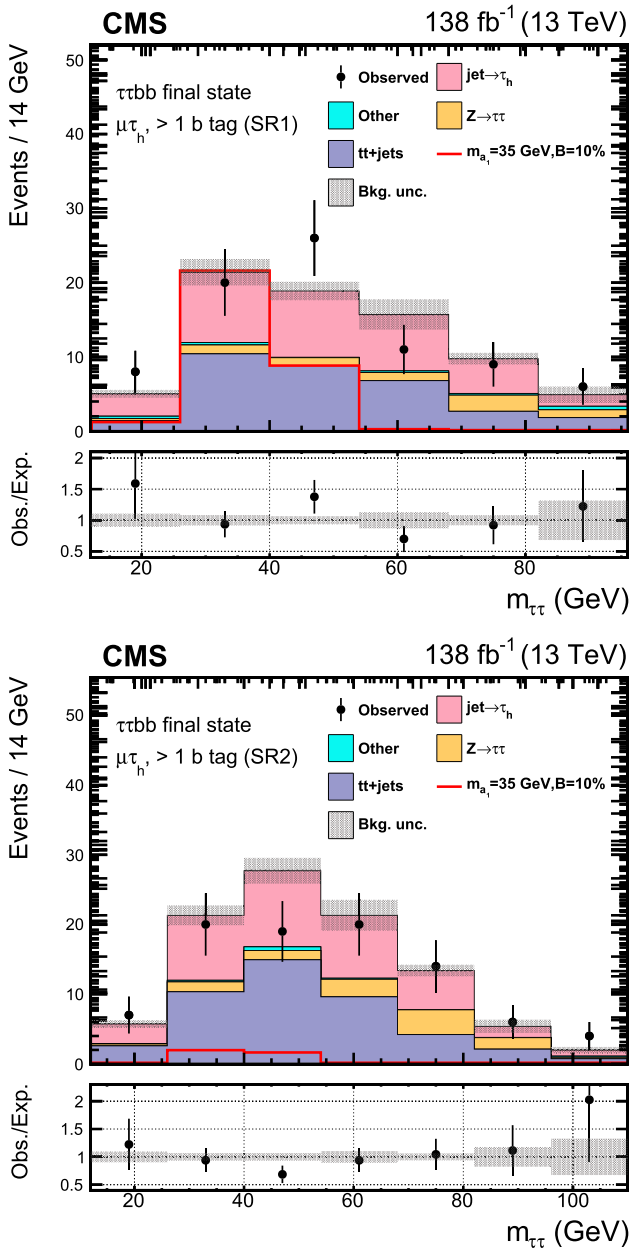


Fig. 8 Post-fit distributions of the $m_{\tau\tau}$ for the $\mu\tau_h$ channel signal regions in events with at least two b tagged jets: SR1 (upper) and SR2 (lower). The shape of the $H \rightarrow a_1 a_1$ signal, where $m_{a_1} = 35$ GeV, is indicated assuming $\mathcal{B}(H \rightarrow a_1 a_1 \rightarrow \tau\tau bb)$ to be 10%

ciated with the background model are evaluated by means of the discrete profiling method as described earlier and contribute to the statistical uncertainty of the result. Depending on the signal mass hypothesis, they constitute about 10–25% of the total uncertainty in the $\mu\mu bb$ results. Contributions from uncertainties in the signal efficiency and acceptance are significantly smaller. In the following, details are provided for several sources of uncertainties.

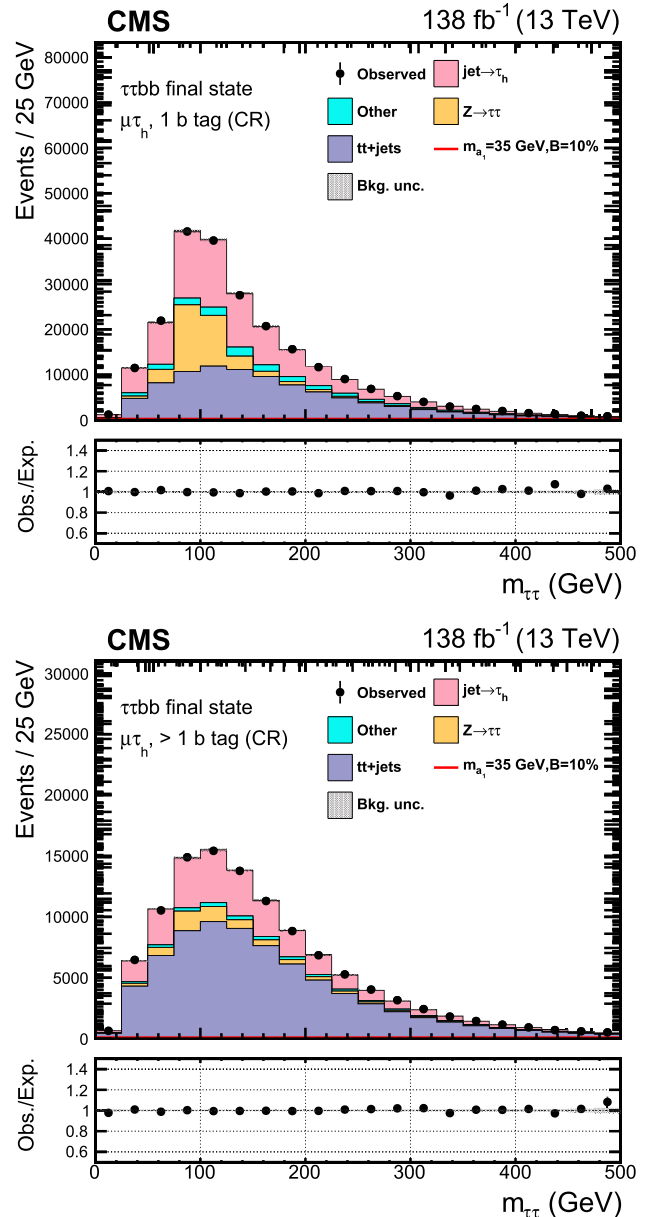


Fig. 9 Post-fit distributions of the $m_{\tau\tau}$ for the $\mu\tau_h$ channel control regions in events with exactly one b tagged jet and at least two b tagged jets (lower). The contamination from the $H \rightarrow a_1 a_1$ signal, where $m_{a_1} = 35$ GeV, is barely visible assuming $\mathcal{B}(H \rightarrow a_1 a_1 \rightarrow \tau\tau bb)$ to be 10%

All uncertainties are included as nuisance parameters in the final fit for the signal extraction. Uncertainties affecting the event yields in categories, i.e., normalization uncertainties, are assigned via multiplicative corrections, with a log-normal probability density function. In the binned maximum likelihood fit of the $\tau\tau bb$ analysis, nuisance parameters that modify the shapes of the $m_{\tau\tau}$ distributions are assumed to have a Gaussian profile. This means that for every nuisance parameter of this type, two alternate distributions are provided to the fit: one with the distribution resulting from an

increase of the nuisance parameter by one standard deviation and the other with the distribution resulting from a decrease by one standard deviation. The dominant systematic uncertainty is found to be associated with the signal model, followed by the normalization of the QCD multijet background in the $e\mu$ final state and the uncertainties in the $t\bar{t}$ +jets cross section.

Integrated luminosity: the integrated luminosity of the data recorded by CMS for physics analyses is evaluated separately for different years of the Run 2 data taking [87–89]. The uncertainty in the measured integrated luminosity of a given year has a component that is uncorrelated across the years. It amounts to 1.0, 2.0, and 1.5%, for the 2016, 2017, and 2018 periods, respectively. Another component is correlated across all three years and is 0.6% in 2016, 0.9% in 2017, and 2.0% in 2018. Furthermore, the luminosity measurements in 2017–2018 have additional uncertainties, of 0.6 and 0.2%, respectively, that are considered correlated between the two years. The overall uncertainty in integrated luminosity for the 2016–2018 period is 1.6%.

Pileup: the uncertainty associated with the number of pileup interactions per bunch crossing is estimated by varying the total inelastic pp cross section by 4.6% [90], fully correlated across the years.

ECAL timing shift: during the 2016–2017 data-taking periods, a gradual shift in the timing of the ECAL L1 trigger inputs occurred in the forward endcap region, $|\eta| > 2.4$ [91]. This led to a specific inefficiency due to erroneous association of detector readout to the previous bunch crossing in a small fraction of the collision events. A correction to this effect was determined using an unbiased data sample and found to be relevant in events containing high- p_T jets with $2.4 < |\eta| < 3.0$. This correction is applied to simulation and is accompanied by a 20% uncertainty. The uncertainty predominantly affects the VBF category in the $\mu\mu b\bar{b}$ analysis, with a negligible effect on the results in this channel.

Jet energy corrections: the jet energy scale (JES) uncertainties include several sources parameterized as a function of the jet p_T and η [92]. Those variations can modify the content of the selected event sample. They also introduce event migration between categories. In the $\mu\mu b\bar{b}$ analysis, the event p_T^{miss} changes as a result of variations in the jet kinematics whereas in the $\tau\tau b\bar{b}$ analysis, JES uncertainties affect the $m_{\tau\tau}$ distribution. Variations in the expected signal yield are between 15–50% in the $\mu\mu b\bar{b}$ analysis. In the $\tau\tau b\bar{b}$ channel, distributions vary between 10–15% of the nominal. Depending on the source, JES uncertainties are considered as uncorrelated, fully correlated, or partially correlated (50%) across the years. The jet energy resolution is also considered, where the smearing corrections are varied within their uncertainties, uncorrelated across the years.

b tagging: sources of systematic uncertainty that affect the data-to-simulation corrections of the b tagging discrim-

inant distribution are JES, the light flavor or gluon (LF) jet contamination in the b jet sample, the heavy flavor (HF) jet contamination in the LF jet sample, and the statistical fluctuations in data and MC [70]. The JES variations in b tagging are obtained together with the JES uncertainties on jet kinematics and follow the same correlation pattern across the years. The statistical components of the b tagging uncertainties are uncorrelated while the rest are assumed correlated between different periods.

Muon reconstruction: the data-to-simulation correction factors for the muon tracking, reconstruction and selection efficiencies are estimated using a “tag-and-probe” method [93] in DY data and simulated samples. These uncertainties include the pileup dependence of the correction factors and are correlated across the years since common procedural uncertainties are the dominant source. The requirements between the two analyses are slightly different, mainly because of a different impact parameter in $\tau \rightarrow \mu$ decays. The corrections, and therefore associated systematic uncertainties, are applied in bins of muon p_T and $|\eta|$ in the $\mu\mu b\bar{b}$ analysis [63]. In the $\tau\tau b\bar{b}$ analysis, a 2% uncertainty, independent of p_T and η , per muon is used [94] and treated as uncorrelated between simulated and τ -embedded events. The muon momentum scale varies within 0.4–2.7% [63] and is accounted for in systematic uncertainties on the signal and background $m_{\tau\tau}$ distribution. Its impact is found to be negligible in the $\mu\mu b\bar{b}$ analysis.

Electron reconstruction: the electron energy scale uncertainties in $e\mu$ and $e\tau_h$ final states are accounted for using methods outlined in Ref. [95]. The reconstruction and selection efficiencies are accompanied by a 2% uncertainty per electron, independent of p_T and η [64]. Similar to muons, these uncertainties are uncorrelated between simulated and τ -embedded events. Uncertainties in the electron energy scale also affect the shapes of the $m_{\tau\tau}$ distributions and are accounted for.

Hadronically decaying τ lepton reconstruction: in $\mu\tau_h$ and $e\tau_h$ final states, there are uncertainties associated with τ_h identification efficiencies and energy scale corrections where the variations depend on p_T (τ_h) and decay mode, ranging from 3–5% and 0.2–1.1%, respectively. Systematic variations in the selected event yields as well as in the shapes of the distributions are taken into account. Uncertainties are considered uncorrelated across the bins of p_T (τ_h) and different years for the MC [72]. Uncertainties of the same source are treated as 50% correlated between the embedded DY background and simulated samples. For events with a genuine τ_h lepton matched at the generator level, energy scale uncertainties are considered using shape variations. In the case of muons and electrons misidentified as τ_h candidates, energy scale corrections are applied in bins of p_T , η , and decay mode of the misidentified τ_h . These corrections are associated with uncertainties. A 50% correlation is consid-

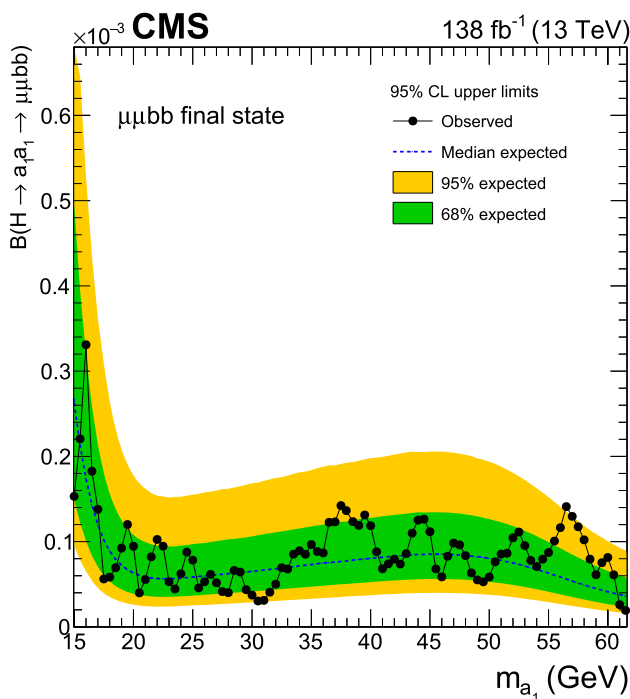


Fig. 10 Observed and expected upper limits at 95% CL on $\mathcal{B}(H \rightarrow a_1 a_1 \rightarrow \mu\mu bb)$ as functions of m_{a_1} . The inner and outer bands indicate the regions containing the distribution of limits located within 68 and 95% confidence intervals, respectively, of the expectation under the background-only hypothesis

ered between the embedded and MC samples for these lepton energy scale uncertainties.

Trigger efficiencies: an uncertainty of 1% is assigned to the HLT efficiency in the $\mu\mu bb$ analysis. In the $\tau\tau bb$ channel, an uncertainty of 2% is applied per single-lepton trigger and 5–10% on the dilepton triggers with a τ_h requirement. Uncertainties associated with trigger efficiencies affect the shape of the distributions in this channel. The shape effects are taken into account in both simulated and embedded backgrounds, where a 50% correlation is considered between the two.

Background estimations in $t\tau bb$ final state: the Z boson p_T reweighting uncertainty in DY samples, which amounts to 10% of the nominal value, is taken as a $m_{\tau\tau}$ shape uncertainty. The embedded samples include a 4% normalization uncertainty [81]. Moreover, shape uncertainties related to tracking efficiencies and contamination from non-DY events in the embedded sample are considered. Since the contribution of the QCD multijet background in the $e\mu$ channel is obtained from a same-sign sideband region with a limited number of events, the validity of the method is tested in independent same-sign SBs. This test results in a 20% normalization uncertainty. The uncertainty in the scale factor between the same-sign SBs and opposite-sign SRs is modeled using shape variations in the fit used to obtain the nominal values. The

misidentification probability, f , of a jet as a τ_h candidate depends on the jet multiplicity. A 20% normalization uncertainty is applied to the estimate of the W+jets and QCD multijet backgrounds due to f being measured in $Z \rightarrow \mu\mu$ events with different jet multiplicities. In addition, shape variations due to different measurements of f are considered.

Limited size of the samples: to account for the limited size of the simulated samples, as well as the data in SBs used to estimate backgrounds, a bin-by-bin statistical uncertainty is considered where a Poisson nuisance parameter per bin is assigned to distributions in those samples [96]. This uncertainty is specific to the $\tau\tau bb$ analysis.

Modeling uncertainties: a total uncertainty of 3.6% is assigned to the sum of the ggF and VBF Higgs boson production cross sections [22] predicted by the SM and used to describe the upper limits on $\mathcal{B}(H \rightarrow a_1 a_1 \rightarrow \mu\mu bb/\tau\tau bb)$. It includes uncertainties from the perturbative QCD calculations, PDFs, and α_S . In the $\tau\tau bb$ analysis, PDF and α_S uncertainties are considered for simulated backgrounds, namely: 4.2% for tt+jets, 5% for Diboson, and 5% for single top quark processes. These uncertainties are obtained following the PDF4LHC prescription [97]. To account for variations in the signal acceptance in both channels, the renormalization and factorization scales are doubled and halved simultaneously in simulation. In addition, the eigenvectors of the NNPDF3.1 PDF set are varied within their uncertainties in the final fit. The value of α_S , computed at the energy scale of the Z boson mass, is also varied within its uncertainty in the PDF set. For the parton shower simulation, uncertainties are separately assessed for initial- and final-state radiation, by varying the respective scales up and down by factors of two. Using the same model assumptions and procedures, the aforementioned uncertainties are considered fully correlated across the data-taking years.

9 Results

No excess of events over the expected SM backgrounds is observed in either of the $\mu\mu bb$ and $\tau\tau bb$ channels. Upper limits are placed, at 95% CL, on $\mathcal{B}(H \rightarrow a_1 a_1 \rightarrow \ell\ell bb)$ as a function of m_{a_1} , with ℓ being either a τ lepton or muon. The two final states are combined to set upper limits on $\mathcal{B}(H \rightarrow a_1 a_1)$, assuming fixed decay fractions of a_1 . The branching fraction $\mathcal{B}(a_1 \rightarrow ff)$ depends on the 2HDM+S parameters, where f indicates either muon, b quark, or τ lepton. Since the results in both channels are statistically limited, the combination mostly benefits from the additional data. The combined results are still dominated by the statistical uncertainties. At $m_{a_1} = 35$ GeV, all systematic uncertainties amount to about 6% of the total uncertainty, with the dominant contributions corresponding to JES in the $\mu\mu bb$ channel, followed by the theoretical uncertainties in the signal, and

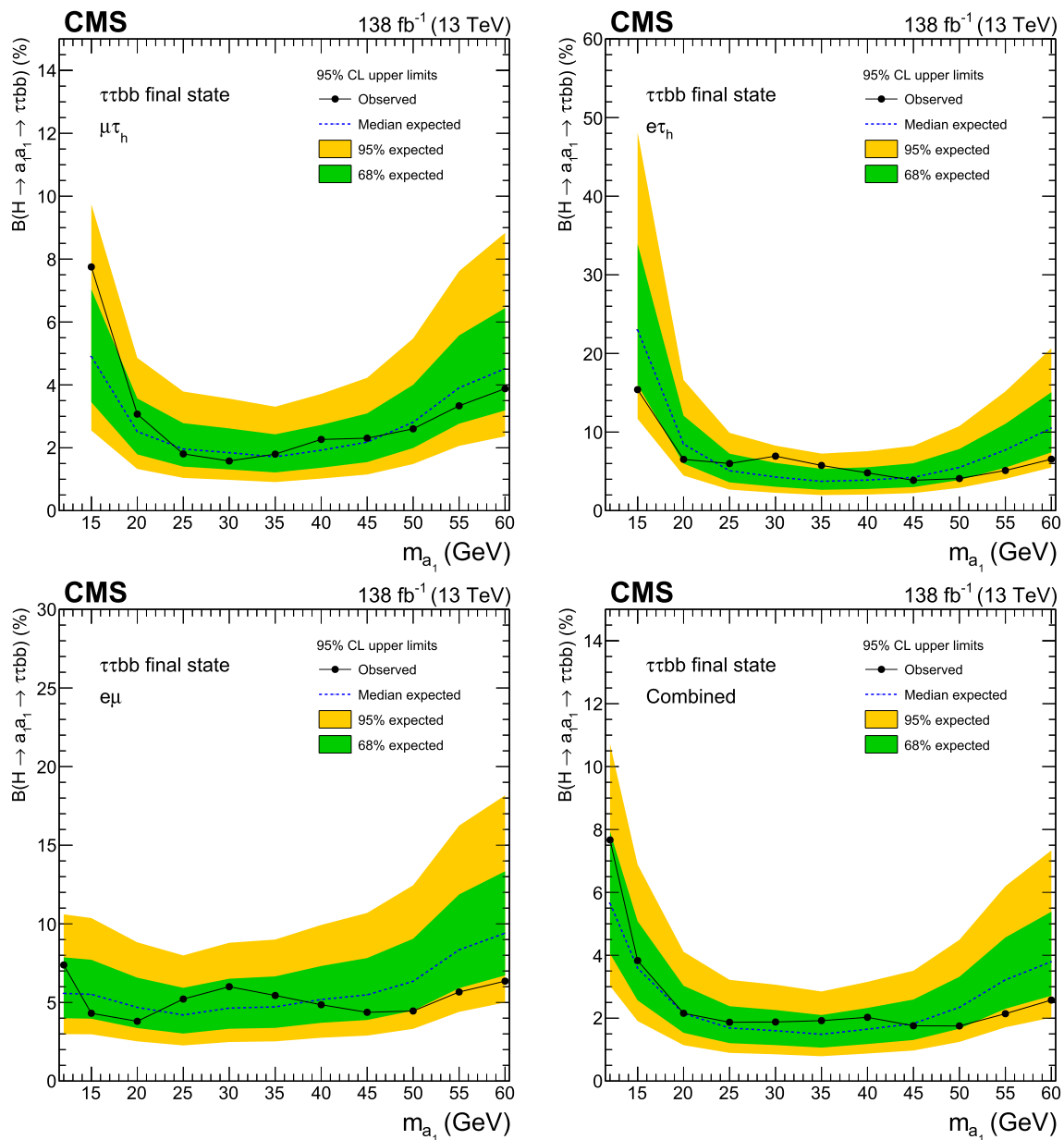


Fig. 11 Observed and expected 95% CL exclusion limits on $\mathcal{B}(H \rightarrow a_1 a_1 \rightarrow \tau\tau bb)$ in percent, for the (upper left) $\mu\tau_h$, (upper right) $e\tau_h$, (lower left) $e\mu$ channels, and (lower right) for the combination of all the channels

finally the uncertainties in the QCD multijet backgrounds in the $e\mu$ final state of the $\tau\tau bb$ analysis.

Figure 10 shows the upper limits on $\mathcal{B}(H \rightarrow a_1 a_1 \rightarrow \mu\mu bb)$ at 95% CL, assuming SM predictions for the Higgs boson production cross section. The $\mu\mu bb$ search is optimized for m_{a_1} values between 15 and 60 GeV, with signal sensitivity falling rapidly below $m_{a_1} = 20$ GeV. This is mainly because the two b jets start to merge as a result of a higher momentum for a_1 . At 95% CL, the observed upper limits are $(0.17\text{--}3.3) \times 10^{-4}$ for the mass range 15 to 62.5 GeV, while the expected limits are $(0.35\text{--}2.6) \times 10^{-4}$.

Figure 11 shows the observed and expected 95% CL upper limits on $\mathcal{B}(H \rightarrow a_1 a_1 \rightarrow \tau\tau bb)$ as functions of m_{a_1} . Only the $e\mu$ channel provides sensitivity to the 12 GeV mass point, as in this channel the baseline selection on the ΔR between the two τ candidates is the lowest. For small m_{a_1} values, the decay products appear as boosted and may not be reconstructed as two separate objects. The low ΔR requirement allows a selection of more signal events where the two τ candidates are close to each other. The $\mu\tau_h$ final state is the most sensitive, where limits as low as around 1.8% (1.7%) are observed (expected) in the intermediate mass range at $m_{a_1} = 35$ GeV. Combining all final states in the $\tau\tau bb$ chan-

nel, observed limits on the branching fraction are found to be in the range 1.7–7.7%, for a pseudoscalar mass between 12 and 60 GeV, with corresponding expected limits in the range 1.5–5.7% at 95% CL.

Figure 12 shows the observed and expected limits at 95% CL on $\mathcal{B}(H \rightarrow a_1 a_1 \rightarrow \ell \ell b \bar{b})$, where ℓ stands for muons or τ leptons. Using decay width expression from Ref. [86], the signal strength of each channel is scaled with a type and $\tan \beta$ independent factor to obtain this limit in the context of 2HDM+S models. The observed and expected ranges are 0.6–7.7% and 0.8–5.7% respectively, depending on m_{a_1} .

The combined branching fraction $\mathcal{B}(H \rightarrow a_1 a_1)$ is obtained upon reinterpretation of the $\mu\mu b \bar{b}$ and $\tau\tau b \bar{b}$ results in different types of 2HDM+S and $\tan \beta$ values for $15 < m_{a_1} < 60$ GeV, illustrated in Fig. 13. Upper limits in the range 5–23% are observed at 95% CL for all Type II scenarios with $\tan \beta > 1.0$. The tightest constraint is obtained for the Type III scenario with $\tan \beta = 2.0$. At 95% CL, the observed upper limits on the combined branching fraction are in the range 1–7%, with a similar range for the expected upper limits. For the Type IV scenario, the observed upper limits on $\mathcal{B}(H \rightarrow a_1 a_1)$ at 95% CL are between about 3 and 15% for $\tan \beta = 0.5$, with corresponding expected limits between about 3 and 11%.

The allowed values of $\tan \beta$ and m_{a_1} are shown in Fig. 14 in the context of Type III and Type IV 2HDM+S. The dashed contours represent the upper limits at 95% CL on Higgs boson to pseudoscalar decays, assuming the branching fraction to be either 100 or 16%. Here 16% corresponds to the combined upper limit on Higgs boson to BSM particle decays obtained from previous Run 2 results [16].

10 Summary

A search for an exotic decay of the 125 GeV Higgs boson (H) to a pair of light pseudoscalar bosons (a_1) in the final state with two b quarks and two muons or two τ leptons has been presented. The results are based on a data sample of proton–proton collisions corresponding to an integrated luminosity of 138 fb^{-1} , accumulated by the CMS experiment at the LHC during Run 2 at a center-of-mass energy of 13 TeV. Final states with at least one leptonic τ decay are studied in the $\tau\tau b \bar{b}$ channel, excluding those with two muons or two electrons. The results show significant improvement, with respect to the earlier CMS analyses at 13 TeV, beyond what is merely expected from the increase in the size of the data sample. A more thorough analysis of the signal properties using a single discriminating variable improves the $\mu\mu b \bar{b}$ analysis, while the $\tau\tau b \bar{b}$ analysis gains from a deep neural network based signal categorization. No significant excess in the data over the standard model backgrounds is observed. Upper limits are set, at 95% confi-

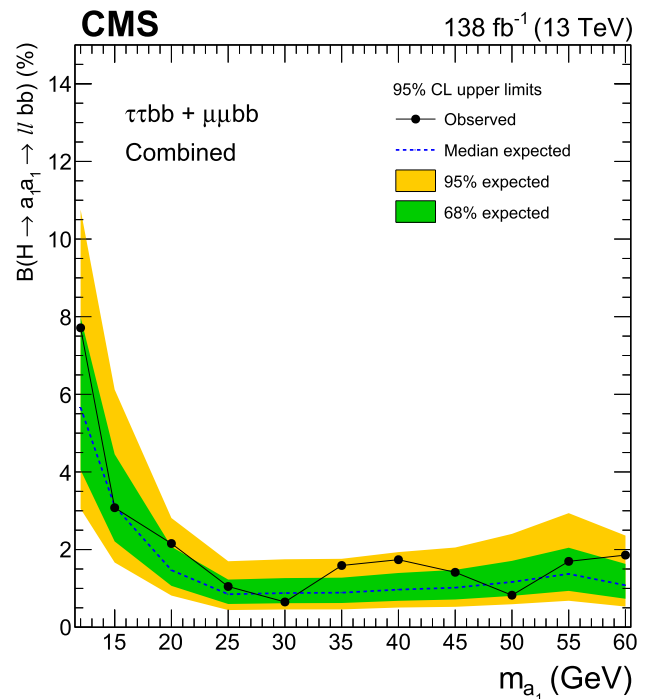


Fig. 12 Observed and expected 95% CL upper limits on $\mathcal{B}(H \rightarrow a_1 a_1 \rightarrow \ell \ell b \bar{b})$ in %, where ℓ stands for muons or τ leptons, obtained from the combination of the $\mu\mu b \bar{b}$ and $\tau\tau b \bar{b}$ channels. The results are obtained as functions of m_{a_1} for 2HDM+S models, independent of the type and $\tan \beta$ parameter

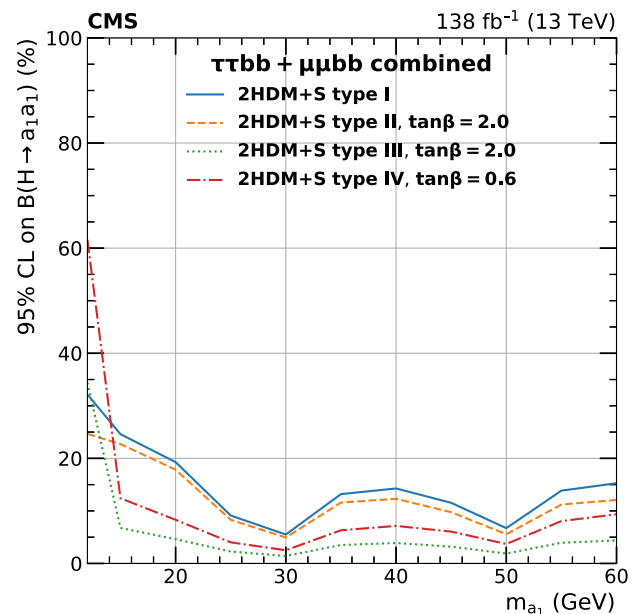


Fig. 13 Observed and expected 95% CL upper limits on $\mathcal{B}(H \rightarrow a_1 a_1)$ in %, obtained from the combination of the $\mu\mu b \bar{b}$ and $\tau\tau b \bar{b}$ channels. The results are obtained as functions of m_{a_1} for 2HDM+S Type I (independent of $\tan \beta$), Type II ($\tan \beta = 2.0$), Type III ($\tan \beta = 2.0$), and Type IV ($\tan \beta = 0.6$), respectively

dence level, on branching fractions $\mathcal{B}(H \rightarrow a_1 a_1 \rightarrow \mu\mu b \bar{b})$ and $\mathcal{B}(H \rightarrow a_1 a_1 \rightarrow \tau\tau b \bar{b})$, in the $\mu\mu b \bar{b}$ and $\tau\tau b \bar{b}$ analyses, respectively. Both analyses provide the most stringent

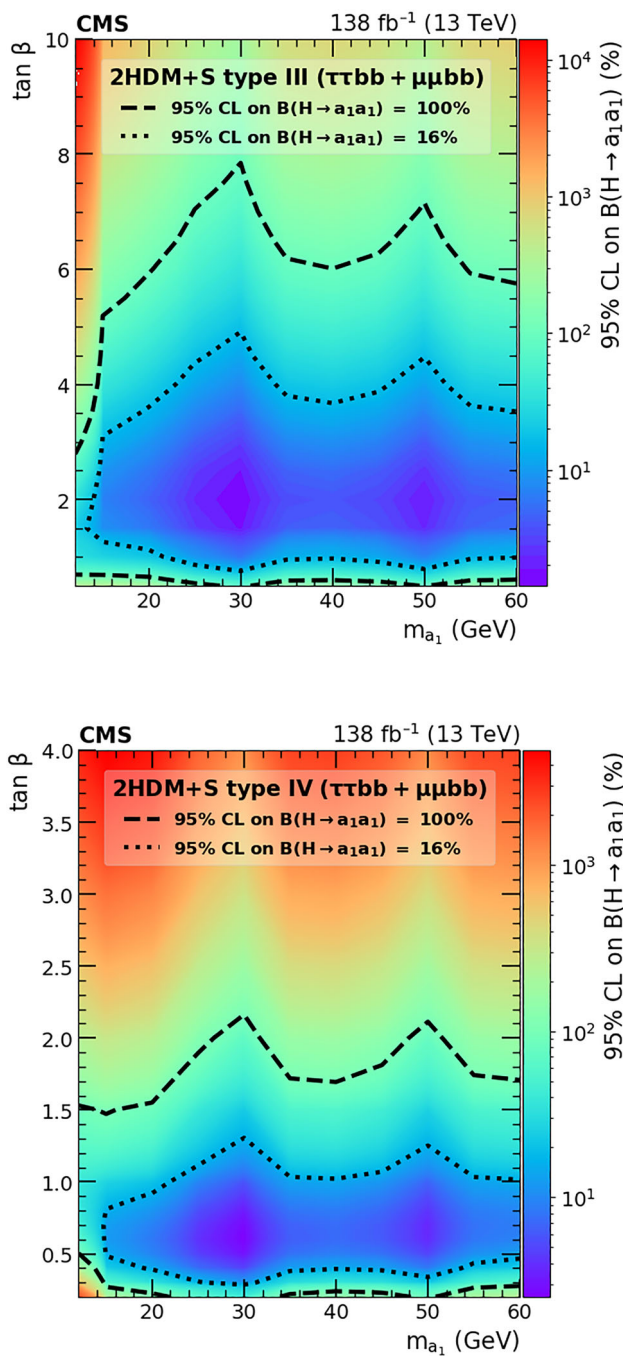


Fig. 14 Observed 95% CL upper limits on $\mathcal{B}(H \rightarrow a_1 a_1)$ in %, for the combination of the $\mu\mu b\bar{b}$ and $\tau\tau b\bar{b}$ channels for Type III (upper) and Type IV (lower) 2HDM+S in the $\tan \beta$ vs. m_{a_1} parameter space. The limits are calculated in a grid of 5 GeV in m_{a_1} and 0.1–0.5 in $\tan \beta$, interpolating the points in between. The contours corresponding to branching fractions of 100 and 16% are drawn using dashed lines, where 16% refers to the combined upper limit on Higgs boson to undetected particle decays from previous Run 2 results [16]. All points inside the contour are allowed within that upper limit

expected limits to date. In the $\mu\mu b\bar{b}$ channel, the observed limits are in the range $(0.17\text{--}3.3) \times 10^{-4}$ for a pseudoscalar mass, m_{a_1} , between 15 and 62.5 GeV. Combining all final

states in the $\tau\tau b\bar{b}$ channel, limits are observed to be in the range 1.7–7.7% for m_{a_1} between 12 and 60 GeV. By combining the $\mu\mu b\bar{b}$ and $\tau\tau b\bar{b}$ channels, upper limits are set on the branching fraction $\mathcal{B}(H \rightarrow a_1 a_1 \rightarrow \ell\ell b\bar{b})$, where ℓ stands for muons or τ leptons. The observed upper limits range between 0.6 and 7.7% depending on the m_{a_1} . The results can also be interpreted in different types of 2HDM+S models. For m_{a_1} values between 15 and 60 GeV, $\mathcal{B}(H \rightarrow a_1 a_1)$ values above 23% are excluded, at 95% confidence level, in most of the Type II scenarios. In Types III and IV, observed upper limits as low as 1 and 3% are obtained, respectively, for $\tan \beta = 2.0$ and 0.5.

Acknowledgements We congratulate our colleagues in the CERN accelerator departments for the excellent performance of the LHC and thank the technical and administrative staffs at CERN and at other CMS institutes for their contributions to the success of the CMS effort. In addition, we gratefully acknowledge the computing centers and personnel of the Worldwide LHC Computing Grid and other centers for delivering so effectively the computing infrastructure essential to our analyses. Finally, we acknowledge the enduring support for the construction and operation of the LHC, the CMS detector, and the supporting computing infrastructure provided by the following funding agencies: SC (Armenia), BMBWF and FWF (Austria); FNRS and FWO (Belgium); CNPq, CAPES, FAPERJ, FAPERGS, and FAPESP (Brazil); MES and BNSF (Bulgaria); CERN; CAS, MoST, and NSFC (China); Minciencias (Colombia); MSES and CSF (Croatia); RIF (Cyprus); SENESCYT (Ecuador); ERC PRG, RVTT3 and MoER TK202 (Estonia); Academy of Finland, MEC, and HIP (Finland); CEA and CNRS/IN2P3 (France); SRNSF (Georgia); BMBF, DFG, and HGF (Germany); GSRI (Greece); NKFIH (Hungary); DAE and DST (India); IPM (Iran); SFI (Ireland); INFN (Italy); MSIP and NRF (Republic of Korea); MES (Latvia); LMTLT (Lithuania); MOE and UM (Malaysia); BUAP, CINVESTAV, CONACYT, LNS, SEP, and UASLP-FAI (Mexico); MOS (Montenegro); MBIE (New Zealand); PAEC (Pakistan); MES and NSC (Poland); FCT (Portugal); MESTD (Serbia); MCIN/AEI and PCTI (Spain); MOSTR (Sri Lanka); Swiss Funding Agencies (Switzerland); MST (Taipei); MHEI and NSTDA (Thailand); TUBITAK and TENMAK (Turkey); NASU (Ukraine); STFC (United Kingdom); DOE and NSF (USA). Individuals have received support from the Marie-Curie program and the European Research Council and Horizon 2020 Grant, contract Nos. 675440, 724704, 752730, 758316, 765710, 824093, 101115353, and COST Action CA16108 (European Union); the Leventis Foundation; the Alfred P. Sloan Foundation; the Alexander von Humboldt Foundation; the Science Committee, project no. 22r1-037 (Armenia); the Belgian Federal Science Policy Office; the Fonds pour la Formation à la Recherche dans l’Industrie et dans l’Agriculture (FRIA-Belgium); the Agentschap voor Innovatie door Wetenschap en Technologie (IWT-Belgium); the F.R.S.-FNRS and FWO (Belgium) under the “Excellence of Science – EOS” – be.h project n. 30820817; the Beijing Municipal Science and Technology Commission, No. Z191100007219010 and Fundamental Research Funds for the Central Universities (China); the Ministry of Education, Youth and Sports (MEYS) of the Czech Republic; the Shota Rustaveli National Science Foundation, grant FR-22-985 (Georgia); the Deutsche Forschungsgemeinschaft (DFG), under Germany’s Excellence Strategy – EXC 2121 “Quantum Universe” – 390833306, and under project number 400140256 - GRK2497; the Hellenic Foundation for Research and Innovation (HFRI), Project Number 2288 (Greece); the Hungarian Academy of Sciences, the New National Excellence Program - ÚNKP, the NKFIH research grants K 124845, K 124850, K 128713, K 128786, K 129058, K 131991, K 133046, K 138136, K 143460, K 143477, 2020-2.2.1-ED-2021-00181, and TKP2021-NKTA-64 (Hungary); the

Council of Science and Industrial Research, India; ICSC – National Research Center for High Performance Computing, Big Data and Quantum Computing, funded by the NextGenerationEU program (Italy); the Latvian Council of Science; the Ministry of Education and Science, project no. 2022/WK/14, and the National Science Center, contracts Opus 2021/41/B/ST2/01369 and 2021/43/B/ST2/01552 (Poland); the Fundação para a Ciência e a Tecnologia, grant CEECIND/01334/2018 (Portugal); the National Priorities Research Program by Qatar National Research Fund; MCIN/AEI/10.13039/501100011033, ERDF “a way of making Europe”, and the Programa Estatal de Fomento de la Investigación Científica y Técnica de Excelencia María de Maeztu, grant MDM-2017-0765 and Programa Severo Ochoa del Principado de Asturias (Spain); the Chulalongkorn Academic into Its 2nd Century Project Advancement Project, and the National Science, Research and Innovation Fund via the Program Management Unit for Human Resources and Institutional Development, Research and Innovation, grant B37G660013 (Thailand); the Kavli Foundation; the Nvidia Corporation; the SuperMicro Corporation; the Welch Foundation, contract C-1845; and the Weston Havens Foundation (USA).

Data availability This manuscript has associated data in a data repository. [Author’s comment: Release and preservation of data used by the CMS Collaboration as the basis for publications is guided by the CMS policy as stated in “<https://cms-docdb.cern.ch/cgi-bin/PublicDocDB/RetrieveFile?docid=6032&filename=CMSDataPolicyV1.2.pdf&version=2>”. CMS data preservation, re-use and open access policy.]

Declarations

Conflict of interest The authors declare that they have no conflict of interest.









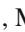










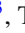










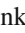

















































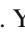




Open Access This article is licensed under a Creative Commons Attribution 4.0 International License, which permits use, sharing, adaptation, distribution and reproduction in any medium or format, as long as you give appropriate credit to the original author(s) and the source, provide a link to the Creative Commons licence, and indicate if changes were made. The images or other third party material in this article are included in the article’s Creative Commons licence, unless indicated otherwise in a credit line to the material. If material is not included in the article’s Creative Commons licence and your intended use is not permitted by statutory regulation or exceeds the permitted use, you will need to obtain permission directly from the copyright holder. To view a copy of this licence, visit <http://creativecommons.org/licenses/by/4.0/>. Funded by SCOAP³.

References













1. ATLAS Collaboration, Observation of a new particle in the search for the Standard Model Higgs boson with the ATLAS detector at the LHC. *Phys. Lett. B* **716**, 1 (2012). <https://doi.org/10.1016/j.physletb.2012.08.020>. arXiv:1207.7214
2. CMS Collaboration, Observation of a new boson at a mass of 125 GeV with the CMS experiment at the LHC. *Phys. Lett. B* **716**, 30 (2012). <https://doi.org/10.1016/j.physletb.2012.08.021>. arXiv:1207.7235
3. CMS Collaboration, Observation of a new boson with mass near 125 GeV in pp collisions at $\sqrt{s} = 7$ and 8 TeV. *JHEP* **06**, 081 (2013). [https://doi.org/10.1007/JHEP06\(2013\)081](https://doi.org/10.1007/JHEP06(2013)081). arXiv:1303.4571
4. F. Englert, R. Brout, Broken symmetry and the mass of gauge vector mesons. *Phys. Rev. Lett.* **13**, 321 (1964). <https://doi.org/10.1103/PhysRevLett.13.321>
5. P.W. Higgs, Broken symmetries, massless particles and gauge fields. *Phys. Lett.* **12**, 132 (1964). [https://doi.org/10.1016/0031-9163\(64\)91136-9](https://doi.org/10.1016/0031-9163(64)91136-9)
6. P.W. Higgs, Broken symmetries and the masses of gauge bosons. *Phys. Rev. Lett.* **13**, 508 (1964). <https://doi.org/10.1103/PhysRevLett.13.508>
7. G.S. Guralnik, C.R. Hagen, T.W.B. Kibble, Global conservation laws and massless particles. *Phys. Rev. Lett.* **13**, 585 (1964). <https://doi.org/10.1103/PhysRevLett.13.585>
8. P.W. Higgs, Spontaneous symmetry breakdown without massless bosons. *Phys. Rev.* **145**, 1156 (1966). <https://doi.org/10.1103/PhysRev.145.1156>
9. T.W.B. Kibble, Symmetry breaking in non-abelian gauge theories. *Phys. Rev.* **155**, 1554 (1967). <https://doi.org/10.1103/PhysRev.155.1554>
10. T.D. Lee, A theory of spontaneous T violation. *Phys. Rev. D* **8**, 1226 (1973). <https://doi.org/10.1103/PhysRevD.8.1226>
11. G.C. Branco et al., Theory and phenomenology of two-Higgs-doublet models. *Phys. Rep.* **516**, 1 (2012). <https://doi.org/10.1016/j.physrep.2012.02.002>. arXiv:1106.0034
12. A. Djouadi, The anatomy of electro-weak symmetry breaking. II. The Higgs bosons in the minimal supersymmetric model. *Phys. Rep.* **459**, 1 (2008). <https://doi.org/10.1016/j.physrep.2007.10.005>. arXiv:hep-ph/0503173
13. T. Robens, T. Stefaniak, Status of the Higgs singlet extension of the standard model after LHC Run 1. *Eur. Phys. J. C* **75**, 104 (2015). <https://doi.org/10.1140/epjc/s10052-015-3323-y>. arXiv:1501.02234
14. T. Robens, T. Stefaniak, J. Wittbrodt, Two-real-scalar-singlet extension of the SM: LHC phenomenology and benchmark scenarios. *Eur. Phys. J. C* **80**, 151 (2020). <https://doi.org/10.1140/epjc/s10052-020-7655-x>. arXiv:1908.08554
15. ATLAS Collaboration, A detailed map of Higgs boson interactions by the ATLAS experiment ten years after the discovery. *Nature* **607**, 52 (2022). <https://doi.org/10.1038/s41586-022-04893-w>. arXiv:2207.00092. [Erratum: <https://doi.org/10.1038/s41586-022-05581-5>]
16. CMS Collaboration, A portrait of the Higgs boson by the CMS experiment ten years after the discovery. *Nature* **607**, 60 (2022). <https://doi.org/10.1038/s41586-022-04892-x>. arXiv:2207.00043
17. D. Curtin et al., Exotic decays of the 125 GeV Higgs boson. *Phys. Rev. D* **90**, 075004 (2014). <https://doi.org/10.1103/PhysRevD.90.075004>. arXiv:1312.4992
18. B. Grzadkowski, P. Osland, Tempered two-Higgs-doublet model. *Phys. Rev. D* **82**, 125026 (2010). <https://doi.org/10.1103/PhysRevD.82.125026>. arXiv:0910.4068
19. A. Drozd, B. Grzadkowski, J.F. Gunion, Y. Jiang, Extending two-Higgs-doublet models by a singlet scalar field—the case for dark matter. *JHEP* **11**, 105 (2014). [https://doi.org/10.1007/JHEP11\(2014\)105](https://doi.org/10.1007/JHEP11(2014)105). arXiv:1408.2106
20. J.E. Kim, H. Nilles, The μ -problem and the strong CP-problem. *Phys. Lett. B* **138**, 150 (1984). [https://doi.org/10.1016/0370-2693\(84\)91890-2](https://doi.org/10.1016/0370-2693(84)91890-2)
21. S. Ramos-Sanchez, The μ -problem, the NMSSM and string theory. *Fortschr. Phys.* **58**, 748 (2010). <https://doi.org/10.1002/prop.201000058>. arXiv:1003.1307
22. D. de Florian et al., Handbook of LHCHiggs cross sections: 4. Deciphering the nature of the Higgs sector. CERN Report CERN-2017-002-M (2016). <https://doi.org/10.23731/CYRM-2017-002>. arXiv:1610.07922
23. ATLAS Collaboration, Search for Higgs boson decays into a pair of pseudoscalar particles in the $bb\mu\mu$ final state with the ATLAS detector in pp collisions at $\sqrt{s} = 13$ TeV. *Phys. Rev. D* **105**, 012006 (2022). <https://doi.org/10.1103/physrevd.105.012006>. arXiv:2110.00313

24. ATLAS Collaboration, Search for Higgs boson decays into a pair of light bosons in the $b\bar{b}\mu\mu$ final state in pp collision at $\sqrt{s} = 13$ TeV with the ATLAS detector. Phys. Lett. B **790**, 1 (2019). <https://doi.org/10.1016/j.physletb.2018.10.073>. arXiv:1807.00539
25. CMS Collaboration, Search for an exotic decay of the Higgs boson to a pair of light pseudoscalars in the final state with two muons and two b quarks in pp collisions at 13 TeV. Phys. Lett. B **795**, 398 (2019). <https://doi.org/10.1016/j.physletb.2019.06.021>. arXiv:1812.06359
26. CMS Collaboration, Search for light bosons in decays of the 125 GeV Higgs boson in proton–proton collisions at $\sqrt{s} = 8$ TeV. JHEP **10**, 076 (2017). [https://doi.org/10.1007/JHEP10\(2017\)076](https://doi.org/10.1007/JHEP10(2017)076). arXiv:1701.02032
27. CMS Collaboration, Search for an exotic decay of the Higgs boson to a pair of light pseudoscalars in the final state with two b quarks and two τ leptons in proton–proton collisions at $\sqrt{s} = 13$ TeV. Phys. Lett. B **785**, 462 (2018). <https://doi.org/10.1016/j.physletb.2018.08.057>. arXiv:1805.10191
28. HEPData record for this analysis (2024). <https://doi.org/10.17182/hepdata.145999>
29. CMS Collaboration, The CMS trigger system. JINST **12**, P01020 (2017). <https://doi.org/10.1088/1748-0221/12/01/P01020>. arXiv:1609.02366
30. CMS Collaboration, The CMS experiment at the CERN LHC. JINST **3**, S08004 (2008). <https://doi.org/10.1088/1748-0221/3/08/S08004>
31. T. Sjöstrand et al., An introduction to PYTHIA 8.2. Comput. Phys. Commun. **191**, 159 (2015). <https://doi.org/10.1016/j.cpc.2015.01.024>. arXiv:1410.3012
32. NNPDF Collaboration, Parton distributions from high-precision collider data. Eur. Phys. J. C **77**, 663 (2017). <https://doi.org/10.1140/epjc/s10052-017-5199-5>. arXiv:1706.00428
33. J. Alwall, S. de Visscher, F. Maltoni, QCD radiation in the production of heavy colored particles at the LHC. JHEP **02**, 017 (2009). <https://doi.org/10.1088/1126-6708/2009/02/017>. arXiv:0810.5350
34. J. Alwall et al., Comparative study of various algorithms for the merging of parton showers and matrix elements in hadronic collisions. Eur. Phys. J. C **53**, 473 (2008). <https://doi.org/10.1140/epjc/s10052-007-0490-5>. arXiv:0706.2569
35. R. Frederix, S. Frixione, Merging meets matching in MC@NLO. JHEP **12**, 061 (2012). [https://doi.org/10.1007/JHEP12\(2012\)061](https://doi.org/10.1007/JHEP12(2012)061). arXiv:1209.6215
36. J. Alwall et al., The automated computation of tree-level and next-to-leading order differential cross sections, and their matching to parton shower simulations. JHEP **07**, 079 (2014). [https://doi.org/10.1007/JHEP07\(2014\)079](https://doi.org/10.1007/JHEP07(2014)079). arXiv:1405.0301
37. P. Skands, S. Carrazza, J. Rojo, Tuning PYTHIA 8.1: the Monash 2013 Tune. Eur. Phys. J. C **74**, 3024 (2014). <https://doi.org/10.1140/epjc/s10052-014-3024-y>. arXiv:1404.5630
38. CMS Collaboration, Extraction and validation of a new set of CMS PYTHIA8 tunes from underlying-event measurements. Eur. Phys. J. C **80**, 4 (2020). <https://doi.org/10.1140/epjc/s10052-019-7499-4>. arXiv:1903.12179
39. GEANT4 Collaboration, GEANT4—a simulation toolkit. Nucl. Instrum. Methods A **506**, 250 (2003). [https://doi.org/10.1016/S0168-9002\(03\)01368-8](https://doi.org/10.1016/S0168-9002(03)01368-8)
40. J. Allison et al., Geant4 developments and applications. IEEE Trans. Nucl. Sci. **53**, 270 (2006). <https://doi.org/10.1109/TNS.2006.869826>
41. CMS Collaboration, Measurements of Higgs boson production in the decay channel with a pair of τ leptons in proton–proton collisions at $\sqrt{s} = 13$ TeV. Eur. Phys. J. C **83**, 562 (2023). <https://doi.org/10.1140/epjc/s10052-023-11452-8>. arXiv:2204.12957
42. P. Nason, A new method for combining NLO QCD with shower Monte Carlo algorithms. JHEP **11**, 040 (2004). <https://doi.org/10.1088/1126-6708/2004/11/040>. arXiv:hep-ph/0409146
43. S. Frixione, P. Nason, C. Oleari, Matching NLO QCD computations with Parton Shower simulations: the POWHEG method. JHEP **11**, 070 (2007). <https://doi.org/10.1088/1126-6708/2007/11/070>. arXiv:0709.2092
44. S. Alioli, P. Nason, C. Oleari, E. Re, A general framework for implementing NLO calculations in shower Monte Carlo programs: the POWHEG BOX. JHEP **06**, 043 (2010). [https://doi.org/10.1007/JHEP06\(2010\)043](https://doi.org/10.1007/JHEP06(2010)043). arXiv:1002.2581
45. S. Alioli et al., Jet pair production in POWHEG. JHEP **04**, 081 (2011). [https://doi.org/10.1007/JHEP04\(2011\)081](https://doi.org/10.1007/JHEP04(2011)081). arXiv:1012.3380
46. M. Czakon et al., Top-pair production at the LHC through NNLO QCD and NLO EW. JHEP **10**, 186 (2017). [https://doi.org/10.1007/JHEP10\(2017\)186](https://doi.org/10.1007/JHEP10(2017)186). arXiv:1705.04105
47. M. Czakon, A. Mitov, Top++: a program for the calculation of the top-pair cross-section at hadron colliders. Comput. Phys. Commun. **185**, 2930 (2014). <https://doi.org/10.1016/j.cpc.2014.06.021>. arXiv:1112.5675
48. M. Botje et al., The PDF4LHC Working Group interim recommendations (2011). arXiv:1101.0538
49. A.D. Martin, W.J. Stirling, R.S. Thorne, G. Watt, Uncertainties on α_s in global PDF analyses and implications for predicted hadronic cross sections. Eur. Phys. J. C **64**, 653 (2009). <https://doi.org/10.1140/epjc/s10052-009-1164-2>. arXiv:0905.3531
50. J. Gao et al., CT10 next-to-next-to-leading order global analysis of QCD. Phys. Rev. D **89**, 033009 (2014). <https://doi.org/10.1103/PhysRevD.89.033009>. arXiv:1302.6246
51. R.D. Ball et al., Parton distributions with LHC data. Nucl. Phys. B **867**, 244 (2013). <https://doi.org/10.1016/j.nuclphysb.2012.10.003>. arXiv:1207.1303
52. J. Campbell, T. Neumann, Z. Sullivan, Single-top-quark production in the t -channel at NNLO. JHEP **02**, 040 (2021). [https://doi.org/10.1007/JHEP02\(2021\)040](https://doi.org/10.1007/JHEP02(2021)040). arXiv:2012.01574
53. PDF4LHC Working Group Collaboration, The PDF4LHC21 combination of global PDF fits for the LHC Run III. J. Phys. G **49**, 080501 (2022). <https://doi.org/10.1088/1361-6471/ac7216>. arXiv:2203.05506
54. K. Melnikov, F. Petriello, Electroweak gauge boson production at hadron colliders through $O(\alpha_s^2)$. Phys. Rev. D **74**, 114017 (2006). <https://doi.org/10.1103/PhysRevD.74.114017>. arXiv:hep-ph/0609070
55. A.D. Martin, W.J. Stirling, R.S. Thorne, G. Watt, Parton distributions for the LHC. Eur. Phys. J. C **63**, 189–285 (2009). <https://doi.org/10.1140/epjc/s10052-009-1072-5>. arXiv:0901.0002
56. S. Alioli, P. Nason, C. Oleari, E. Re, NLO Higgs boson production via gluon fusion matched with shower in POWHEG. JHEP **04**, 002 (2009). <https://doi.org/10.1088/1126-6708/2009/04/002>. arXiv:0812.0578
57. E. Bagnaschi, G. Degrandi, P. Slavich, A. Vicini, Higgs production via gluon fusion in the POWHEG approach in the SM and in the MSSM. JHEP **02**, 088 (2012). [https://doi.org/10.1007/JHEP02\(2012\)088](https://doi.org/10.1007/JHEP02(2012)088). arXiv:1111.2854
58. P. Nason, C. Oleari, NLO Higgs boson production via vector-boson fusion matched with shower in POWHEG. JHEP **02**, 037 (2010). [https://doi.org/10.1007/JHEP02\(2010\)037](https://doi.org/10.1007/JHEP02(2010)037). arXiv:0911.5299
59. G. Luisoni, P. Nason, C. Oleari, F. Tramontano, $HW^\pm/HZ + 0$ and 1 jet at NLO with the POWHEG BOX interfaced to GoSam and their merging within MiNLO. JHEP **10**, 083 (2013). [https://doi.org/10.1007/JHEP10\(2013\)083](https://doi.org/10.1007/JHEP10(2013)083). arXiv:1306.2542
60. H.B. Hartanto, B. Jager, L. Reina, D. Wackerth, Higgs boson production in association with top quarks in the POWHEG BOX. Phys. Rev. D **91**, 094003 (2015). <https://doi.org/10.1103/PhysRevD.91.094003>. arXiv:1501.04498










61. CMS Collaboration, Particle-flow reconstruction and global event description with the CMS detector. *JINST* **12**, P10003 (2017). <https://doi.org/10.1088/1748-0221/12/10/P10003>. [arXiv:1706.04965](https://arxiv.org/abs/1706.04965)
62. CMS Collaboration, Technical proposal for the Phase-II upgrade of the Compact Muon Solenoid. CMS Technical Proposal CERN-LHCC-2015-010, CMS-TDR-15-02 (2015)
63. CMS Collaboration, Performance of the CMS muon detector and muon reconstruction with proton–proton collisions at $\sqrt{s} = 13$ TeV. *JINST* **13**, P06015 (2018). <https://doi.org/10.1088/1748-0221/13/06/P06015>. [arXiv:1804.04528](https://arxiv.org/abs/1804.04528)
64. CMS Collaboration, Electron and photon reconstruction and identification with the CMS experiment at the CERN LHC. *JINST* **16**, P05014 (2021). <https://doi.org/10.1088/1748-0221/16/05/p05014>. [arXiv:2012.06888](https://arxiv.org/abs/2012.06888)
65. M. Cacciari, G.P. Salam, G. Soyez, The anti- k_t jet clustering algorithm. *JHEP* **04**, 063 (2008). <https://doi.org/10.1088/1126-6708/2008/04/063>. [arXiv:0802.1189](https://arxiv.org/abs/0802.1189)
66. M. Cacciari, G.P. Salam, G. Soyez, FastJet user manual. *Eur. Phys. J. C* **72**, 1896 (2012). <https://doi.org/10.1140/epjc/s10052-012-1896-2>. [arXiv:1111.6097](https://arxiv.org/abs/1111.6097)
67. CMS Collaboration, Jet algorithms performance in 13 TeV data. CMS Physics Analysis Summary CMS-PAS-JME-16-003 (2017)
68. CMS Collaboration, Determination of jet energy calibration and transverse momentum resolution in CMS. *JINST* **6**, P11002 (2011). <https://doi.org/10.1088/1748-0221/6/11/P11002>. [arXiv:1107.4277](https://arxiv.org/abs/1107.4277)
69. E. Bols et al., Jet flavour classification using DeepJet. *JINST* **15**, P12012 (2020). <https://doi.org/10.1088/1748-0221/15/12/P12012>. [arXiv:2008.10519](https://arxiv.org/abs/2008.10519)
70. CMS Collaboration, Identification of heavy-flavour jets with the CMS detector in pp collisions at 13 TeV. *JINST* **13**, P05011 (2018). <https://doi.org/10.1088/1748-0221/13/05/P05011>. [arXiv:1712.07158](https://arxiv.org/abs/1712.07158)
71. CMS Collaboration, Performance of the DeepJet b tagging algorithm using 41.9/fb of data from proton–proton collisions at 13 TeV with Phase 1 CMS detector. CMS Detector Performance Note CMS-DP-2018-058 (2018)
72. CMS Collaboration, Performance of reconstruction and identification of τ leptons decaying to hadrons and ν_τ in pp collisions at $\sqrt{s} = 13$ TeV. *JINST* **13**, P10005 (2018). <https://doi.org/10.1088/1748-0221/13/10/P10005>. [arXiv:1809.02816](https://arxiv.org/abs/1809.02816)
73. CMS Collaboration, Identification of hadronic tau lepton decays using a deep neural network. *JINST* **17**, P07023 (2022). <https://doi.org/10.1088/1748-0221/17/07/P07023>. [arXiv:2201.08458](https://arxiv.org/abs/2201.08458)
74. CMS Collaboration, Performance of missing transverse momentum reconstruction in proton–proton collisions at $\sqrt{s} = 13$ TeV using the CMS detector. *JINST* **14**, P07004 (2019). <https://doi.org/10.1088/1748-0221/14/07/P07004>. [arXiv:1903.06078](https://arxiv.org/abs/1903.06078)
75. J. Lever, M. Krzywinski, N. Altman, Principal component analysis. *Nat. Methods* **14**, 641 (2017). <https://doi.org/10.1038/nmeth.4346>
76. CDF Collaboration, Search for neutral Higgs bosons of the minimal supersymmetric standard model decaying to τ pairs in $p\bar{p}$ collisions at $\sqrt{s} = 1.96$ TeV. *Phys. Rev. Lett.* **96**, 011802 (2006). <https://doi.org/10.1103/PhysRevLett.96.011802>. [arXiv:hep-ex/0508051](https://arxiv.org/abs/hep-ex/0508051)
77. L. Bianchini et al., Reconstruction of the Higgs mass in events with Higgs bosons decaying into a pair of tau leptons using matrix element technique. *Nucl. Instrum. Methods A* **862**, 54 (2017). <https://doi.org/10.1016/j.nima.2017.05.001>. [arXiv:1603.05910](https://arxiv.org/abs/1603.05910)
78. P.D. Dauncey, M. Kenzie, N. Wardle, G.J. Davies, Handling uncertainties in background shapes: the discrete profiling method. *JINST* **10**, P04015 (2015). <https://doi.org/10.1088/1748-0221/10/04/P04015>. [arXiv:1408.6865](https://arxiv.org/abs/1408.6865)
79. CMS Collaboration, Observation of the diphoton decay of the Higgs boson and measurement of its properties. *Eur. Phys. J. C* **74**, 3076 (2014). <https://doi.org/10.1140/epjc/s10052-014-3076-z>. [arXiv:1407.0558](https://arxiv.org/abs/1407.0558)
80. ATLAS, CMS Collaboration, Combined measurement of the Higgs boson mass in pp collisions at $\sqrt{s} = 7$ and 8 TeV with the ATLAS and CMS experiments. *Phys. Rev. Lett.* **114**, 191803 (2015). <https://doi.org/10.1103/PhysRevLett.114.191803>. [arXiv:1503.07589](https://arxiv.org/abs/1503.07589)
81. CMS Collaboration, An embedding technique to determine $\tau\tau$ backgrounds in proton–proton collision data. *JINST* **14**, P06032 (2019). <https://doi.org/10.1088/1748-0221/14/06/P06032>. [arXiv:1903.01216](https://arxiv.org/abs/1903.01216)
82. M.J. Oreglia, A study of the reactions $\psi' \rightarrow \gamma\gamma\psi$. PhD thesis, Stanford University (1980). SLAC Report SLAC-R-236
83. T. Junk, Confidence level computation for combining searches with small statistics. *Nucl. Instrum. Methods A* **434**, 435 (1999). [https://doi.org/10.1016/S0168-9002\(99\)00498-2](https://doi.org/10.1016/S0168-9002(99)00498-2). [arXiv:hep-ex/9902006](https://arxiv.org/abs/hep-ex/9902006)
84. A.L. Read, Presentation of search results: the CL_s technique. *J. Phys. G* **28**, 2693 (2002). <https://doi.org/10.1088/0954-3899/28/10/313>
85. G. Cowan, K. Cranmer, E. Gross, O. Vitells, Asymptotic formulae for likelihood-based tests of new physics. *Eur. Phys. J. C* **71**, 1554 (2011). <https://doi.org/10.1140/epjc/s10052-011-1554-0>. [arXiv:1007.1727](https://arxiv.org/abs/1007.1727). [Erratum: <https://doi.org/10.1140/epjc/s10052-013-2501-z>]
86. U. Haisch, J.F. Kamenik, A. Malinauskas, M. Spira, Collider constraints on light pseudoscalars. *JHEP* **03**, 178 (2018). [https://doi.org/10.1007/JHEP03\(2018\)178](https://doi.org/10.1007/JHEP03(2018)178). [arXiv:1802.02156](https://arxiv.org/abs/1802.02156)
87. CMS Collaboration, Precision luminosity measurement in proton–proton collisions at $\sqrt{s} = 13$ TeV in 2015 and 2016 at CMS. *Eur. Phys. J. C* **81**, 800 (2021). <https://doi.org/10.1140/epjc/s10052-021-09538-2>. [arXiv:2104.01927](https://arxiv.org/abs/2104.01927)
88. CMS Collaboration, CMS luminosity measurement for the 2017 data-taking period at $\sqrt{s} = 13$ TeV. CMS Physics Analysis Summary CMS-PAS-LUM-17-004 (2018)
89. CMS Collaboration, CMS luminosity measurement for the 2018 data-taking period at $\sqrt{s} = 13$ TeV. CMS Physics Analysis Summary CMS-PAS-LUM-18-002 (2019)
90. CMS Collaboration, Measurement of the inelastic proton–proton cross section at $\sqrt{s} = 13$ TeV. *JHEP* **07**, 161 (2018). [https://doi.org/10.1007/JHEP07\(2018\)161](https://doi.org/10.1007/JHEP07(2018)161). [arXiv:1802.02613](https://arxiv.org/abs/1802.02613)
91. CMS Collaboration, Performance of the CMS Level-1 trigger in proton–proton collisions at $\sqrt{s} = 13$ TeV. *JINST* **15**, P10017 (2020). <https://doi.org/10.1088/1748-0221/15/10/P10017>. [arXiv:2006.10165](https://arxiv.org/abs/2006.10165)
92. CMS Collaboration, Jet energy scale and resolution in the CMS experiment in pp collisions at 8 TeV. *JINST* **12**, P02014 (2017). <https://doi.org/10.1088/1748-0221/12/02/P02014>. [arXiv:1607.03663](https://arxiv.org/abs/1607.03663)
93. CMS Collaboration, Measurement of the inclusive W and Z production cross sections in pp collisions at $\sqrt{s} = 7$ TeV. *JHEP* **10**, 132 (2011). [https://doi.org/10.1007/JHEP10\(2011\)132](https://doi.org/10.1007/JHEP10(2011)132). [arXiv:1107.4789](https://arxiv.org/abs/1107.4789)
94. CMS Collaboration, Measurement of the inclusive and differential Higgs boson production cross sections in the decay mode to a pair of τ leptons in pp collisions at $\sqrt{s} = 13$ TeV. *Phys. Rev. Lett.* **128**, 081805 (2022). <https://doi.org/10.1103/PhysRevLett.128.081805>. [arXiv:2107.11486](https://arxiv.org/abs/2107.11486)
95. CMS Collaboration, Performance of electron reconstruction and selection with the CMS detector in proton–proton collisions at $\sqrt{s} = 8$ TeV. *JINST* **10**, P06005 (2015). <https://doi.org/10.1088/1748-0221/10/06/P06005>. [arXiv:1502.02701](https://arxiv.org/abs/1502.02701)
96. R.J. Barlow, C. Beeston, Fitting using finite Monte Carlo samples. *Comput. Phys. Commun.* **77**, 219 (1993). [https://doi.org/10.1016/0010-4655\(93\)90005-W](https://doi.org/10.1016/0010-4655(93)90005-W)
97. J. Butterworth et al., PDF4LHC recommendations for LHC Run II. *J. Phys. G* **43**, 023001 (2016). <https://doi.org/10.1088/0954-3899/43/2/023001>. [arXiv:1510.03865](https://arxiv.org/abs/1510.03865)

CMS Collaboration**Yerevan Physics Institute, Yerevan, Armenia**A. Hayrapetyan, A. Tumasyan ¹**Institut für Hochenergiephysik, Vienna, Austria**W. Adam , J. W. Andrejkovic , T. Bergauer , S. Chatterjee , K. Damanakis , M. Dragicevic ,
A. Escalante Del Valle , P. S. Hussain , M. Jeitler ², N. Krammer , D. Liko , I. Mikulec ²,
R. Schöfbeck , D. Schwarz , M. Sonawane , S. Templ , W. Waltenberger , C.-E. Wulz ²**Universiteit Antwerpen, Antwerp, Belgium**M. R. Darwish ³, T. Janssen , P. Van Mechelen **Vrije Universiteit Brussel, Brussels, Belgium**E. S. Bols , J. D'Hondt , S. Dansana , A. De Moor , M. Delcourt , H. El Faham , S. Lowette , I. Makarenko ,
D. Müller , A. R. Sahasransu , S. Tavernier , M. Tytgat ⁴, S. Van Putte , D. Vannerom **Université Libre de Bruxelles, Brussels, Belgium**B. Clerbaux , G. De Lentdecker , L. Favart , D. Hohov , J. Jaramillo , A. Khalilzadeh , K. Lee ,
M. Mahdavihorrani , A. Malara , S. Paredes , L. Pétre , N. Postiau , L. Thomas , M. Vanden Bemden ,
C. Vander Velde , P. Vanlaer **Ghent University, Ghent, Belgium**M. De Coen , D. Dobur , Y. Hong , J. Knolle , L. Lambrecht , G. Mestdach , C. Rendón , A. Samalan ,
K. Skovpen , N. Van Den Bossche , L. Wezenbeek **Université Catholique de Louvain, Louvain-la-Neuve, Belgium**A. Benecke , G. Bruno , C. Caputo , C. Delaere , I. S. Donertas , A. Giammanco , K. Jaffel , Sa. Jain ,
V. Lemaitre , J. Lidrych , P. Mastrapasqua , K. Mondal , T. T. Tran , S. Wertz **Centro Brasileiro de Pesquisas Físicas, Rio de Janeiro, Brazil**G. A. Alves , E. Coelho , C. Hensel , T. Menezes De Oliveira , A. Moraes , P. Rebello Teles , M. Soeiro **Universidade do Estado do Rio de Janeiro, Rio de Janeiro, Brazil**W. L. Aldá Júnior , M. Alves Gallo Pereira , M. Barroso Ferreira Filho , H. Brandao Malbouisson , W. Carvalho ,
J. Chinellato ⁵, E. M. Da Costa , G. G. Da Silveira ⁶, D. De Jesus Damiao , S. Fonseca De Souza , J. Martins ⁷,
C. Mora Herrera , K. Mota Amarilo , L. Mundim , H. Nogima , A. Santoro , S. M. Silva Do Amaral ,
A. Sznajder , M. Thiel , A. Vilela Pereira **Universidade Estadual Paulista, Universidade Federal do ABC, São Paulo, Brazil**C. A. Bernardes ⁶, L. Calligaris , T. R. Fernandez Perez Tomei , E. M. Gregores , P. G. Mercadante ,
S. F. Novaes , B. Orzari , Sandra S. Padula **Institute for Nuclear Research and Nuclear Energy, Bulgarian Academy of Sciences, Sofia, Bulgaria**A. Aleksandrov , G. Antchev , R. Hadjiiska , P. Iaydjiev , M. Misheva , M. Shopova , G. Sultanov **University of Sofia, Sofia, Bulgaria**A. Dimitrov , T. Ivanov , L. Litov , B. Pavlov , P. Petkov , A. Petrov , E. Shumka **Instituto De Alta Investigación, Universidad de Tarapacá, Casilla 7 D, Arica, Chile**S. Keshri , S. Thakur **Beihang University, Beijing, China**T. Cheng , Q. Guo , T. Javaid , M. Mittal , L. Yuan **Department of Physics, Tsinghua University, Beijing, China**G. Bauer ^{8,9}, Z. Hu , K. Yi ^{8,10}

Institute of High Energy Physics, Beijing, China

G. M. Chen ¹¹, H. S. Chen ¹¹, M. Chen ¹¹, F. Iemmi , C. H. Jiang, A. Kapoor ¹², H. Liao , Z.-A. Liu ¹³, F. Monti , M. A. Shahzad¹¹, R. Sharma ¹⁴, J. N. Song¹³, J. Tao , C. Wang¹¹, J. Wang , Z. Wang¹¹, H. Zhang 

State Key Laboratory of Nuclear Physics and Technology, Peking University, Beijing, China

A. Agapitos , Y. Ban , A. Levin , C. Li , Q. Li , X. Lyu, Y. Mao, S. J. Qian , X. Sun , D. Wang , H. Yang, C. Zhou 




Sun Yat-Sen University, Guangzhou, China

Z. You 

University of Science and Technology of China, Hefei, China

N. Lu 

Institute of Modern Physics and Key Laboratory of Nuclear Physics and Ion-beam Application (MOE)-Fudan University, Shanghai, China

X. Gao ¹⁵, D. Leggat, H. Okawa , Y. Zhang 

Zhejiang University, Hangzhou, Zhejiang, China

Z. Lin , C. Lu , M. Xiao 


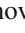
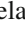
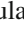
Universidad de Los Andes, Bogotá, Colombia

C. Avila , D. A. Barbosa Trujillo, A. Cabrera , C. Florez , J. Fraga , J. A. Reyes Vega

Universidad de Antioquia, Medellín, Colombia

J. Mejia Guisao , F. Ramirez , M. Rodriguez , J. D. Ruiz Alvarez 

Faculty of Electrical Engineering, Mechanical Engineering and Naval Architecture, University of Split, Split, Croatia

D. Giljanovic , N. Godinovic , D. Lelas , A. Sculac 

Faculty of Science, University of Split, Split, Croatia

M. Kovac , T. Sculac 




Institute Rudjer Boskovic, Zagreb, Croatia

P. Bargassa , V. Brigljevic , B. K. Chitroda , D. Ferencek , S. Mishra , A. Starodumov ¹⁶, T. Susa 

University of Cyprus, Nicosia, Cyprus

A. Attikis , K. Christoforou , S. Konstantinou , J. Mousa , C. Nicolaou, F. Ptochos , P. A. Razis , H. Rykaczewski, H. Saka , A. Stepenov 


Charles University, Prague, Czech Republic

M. Finger , M. Finger Jr. , A. Kveton 

Escuela Politecnica Nacional, Quito, Ecuador

E. Ayala 



Universidad San Francisco de Quito, Quito, Ecuador

E. Carrera Jarrin 

Academy of Scientific Research and Technology of the Arab Republic of Egypt, Egyptian Network of High Energy Physics, Cairo, Egypt

S. Elgammal¹⁷, A. Ellithi Kamel¹⁸

Center for High Energy Physics (CHEP-FU), Fayoum University, El-Fayoum, Egypt

A. Lotfy , M. A. Mahmoud 

















National Institute of Chemical Physics and Biophysics, Tallinn, Estonia

R. K. Dewanjee ¹⁹, K. Ehataht , M. Kadastik, T. Lange , S. Nandan , C. Nielsen , J. Pata , M. Raidal , L. Tani , C. Veelken 

Department of Physics, University of Helsinki, Helsinki, Finland

H. Kirschenmann , K. Osterberg , M. Voutilainen 



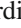











Helsinki Institute of Physics, Helsinki, Finland

S. Bharthuar , E. Brücken , F. Garcia , J. Havukainen , K. T. S. Kallonen , M. S. Kim , R. Kinnunen, T. Lampén , K. Lassila-Perini , S. Lehti , T. Lindén , M. Lotti, L. Martikainen , M. Myllymäki , M. M. Rantanen , H. Siikonen , E. Tuominen , J. Tuominiemi 

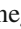





























Lappeenranta-Lahti University of Technology, Lappeenranta, Finland

P. Luukka , H. Petrow , T. Tuuva[†]

IRFU, CEA, Université Paris-Saclay, Gif-sur-Yvette, France

M. Besancon , F. Couderc , M. Dejardin , D. Denegri, J. L. Faure, F. Ferri , S. Ganjour , P. Gras , G. Hamel de Monchenault , V. Lohezic , J. Malcles , J. Rander, A. Rosowsky , M. Ö. Sahin , A. Savoy-Navarro ²⁰, P. Simkina , M. Titov 

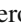
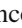






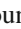

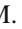

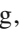




Laboratoire Leprince-Ringuet, CNRS/IN2P3, Ecole Polytechnique, Institut Polytechnique de Paris, Palaiseau, France

C. Baldenegro Barrera , F. Beaudette , A. Buchot Perraguin , P. Busson , A. Cappati , C. Charlot , F. Damas , O. Davignon , A. De Wit , G. Falmagne , B. A. Fontana Santos Alves , S. Ghosh , A. Gilbert , R. Granier de Cassagnac , A. Hakimi , B. Harikrishnan , L. Kalipoliti , G. Liu , J. Motta , M. Nguyen , C. Ochando , L. Portales , R. Salerno , U. Sarkar , J. B. Sauvan , Y. Sirois , A. Tarabini , E. Vernazza , A. Zabi , A. Zghiche 




Université de Strasbourg, CNRS, IPHC UMR 7178, Strasbourg, France

J.-L. Agram ²¹, J. Andrea , D. Appar , D. Bloch , J.-M. Brom , E. C. Chabert , C. Collard , S. Falke , U. Goerlach , C. Grimault, R. Haeberle , A.-C. Le Bihan , M. A. Sessini , P. Van Hove 



Institut de Physique des 2 Infinis de Lyon (IP2I), Villeurbanne, France

S. Beauceron , B. Blancon , G. Boudoul , N. Chanon , J. Choi , D. Contardo , P. Depasse , C. Dozen ²², H. El Mamouni, J. Fay , S. Gascon , M. Gozevitch , C. Greenberg, G. Grenier , B. Ille , I. B. Laktineh, M. Lethuillier , L. Mirabito, S. Perries, M. Vander Donckt , P. Verdier , J. Xiao 








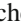





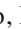













Georgian Technical University, Tbilisi, Georgia

A. Khvedelidze ¹⁶, I. Lomidze , Z. Tsamalaidze ¹⁶



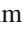

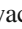




I. Physikalisches Institut, RWTH Aachen University, Aachen, Germany

V. Botta , L. Feld , K. Klein , M. Lipinski , D. Meuser , A. Pauls , N. Röwert , M. Teroerde 








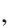

































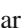
















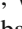


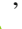
III. Physikalisches Institut A, RWTH Aachen University, Aachen, Germany

S. Diekmann , A. Dodonova , N. Eich , D. Eliseev , F. Engelke , M. Erdmann , P. Fackeldey , B. Fischer , T. Hebbeker , K. Hoepfner , F. Ivone , A. Jung , M. Y. Lee , L. Mastrolorenzo, M. Merschmeyer , A. Meyer , S. Mukherjee , D. Noll , A. Novak , F. Nowotny, A. Pozdnyakov , Y. Rath, W. Redjeb , F. Rehm, H. Reithler , V. Sarkisovi , A. Schmidt , S. C. Schuler, A. Sharma , A. Stein , F. Torres Da Silva De Araujo ²³, L. Vigilante, S. Wiedenbeck , S. Zaleski

III. Physikalisches Institut B, RWTH Aachen University, Aachen, Germany






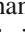

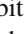


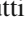
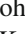





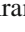

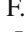



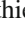



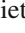
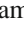
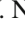




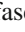


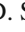


C. Dziwok , G. Flügge , W. Haj Ahmad ²⁴, T. Kress , A. Nowack , O. Pooth , A. Stahl , T. Ziemons , A. Zotz 

Deutsches Elektronen-Synchrotron, Hamburg, Germany





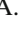
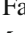




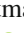
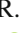




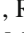
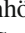

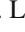



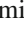

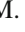

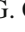



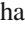

H. Aarup Petersen , M. Aldaya Martin , J. Alimena , S. Amoroso, Y. An , S. Baxter , M. Bayatmakou , H. Becerril Gonzalez , O. Behnke , A. Belvedere , S. Bhattacharya , F. Blekman ²⁵, K. Borrás ²⁶, D. Brunner , A. Campbell , A. Cardini , C. Cheng, F. Colombina , S. Consuegra Rodríguez , G. Correia Silva , M. De Silva , G. Eckerlin, D. Eckstein , L. I. Estevez Banos , O. Filatov , E. Gallo ²⁵, A. Geiser , A. Giraldi , G. Greau, V. Guglielmi , M. Guthoff , A. Hinzmann , A. Jafari ²⁷, L. Jeppe , N. Z. Jomhari , B. Kaech , M. Kasemann , H. Kaveh , C. Kleinwort , R. Kogler , M. Komm , D. Krücker , W. Lange, D. Leyva Pernia , K. Lipka ²⁸, W. Lohmann ²⁹, R. Mankel , I.-A. Melzer-Pellmann , M. Mendizabal Morentin , J. Metwally, A. B. Meyer , G. Milella , A. Musiggiller , A. Nürnberg , Y. Otariid, D. Pérez Adán , E. Ranken , A. Raspereza , B. Ribeiro Lopes , J. Rübenach, A. Saggio , M. Scham ^{30,26}, S. Schnake ²⁶, P. Schütze , C. Schwanenberger ²⁵, D. Selivanova , M. Shchedrolosiev , R. E. Sosa Ricardo , L. P. Sreelatha Pramod , D. Stafford, F. Vazzoler 

A. Ventura Barroso , R. Walsh , Q. Wang , Y. Wen , K. Wichmann, L. Wiens ²⁶, C. Wissing , S. Wuchterl , Y. Yang , A. Zimmermann Castro Santos 

University of Hamburg, Hamburg, Germany

A. Albrecht , S. Albrecht , M. Antonello , S. Bein , L. Benato , M. Bonanomi , P. Connor , M. Eich, K. El Morabit , Y. Fischer , A. Fröhlich, C. Garbers , E. Garutti , A. Grohsjean , M. Hajheidari, J. Haller , H. R. Jabusch , G. Kasieczka , P. Keicher, R. Klanner , W. Korcaric , T. Kramer , V. Kutzner , F. Labe , J. Lange , A. Lobanov , C. Matthies , A. Mehta , L. Moureaux , M. Mrowietz, A. Nigamova , Y. Nissan, A. Paasch , K. J. Pena Rodriguez , T. Quadfasel , B. Raciti , M. Rieger , D. Savoie , J. Schindler , P. Schleper , M. Schröder , J. Schwandt , M. Sommerhalder , H. Stadie , G. Steinbrück , A. Tews, M. Wolf 



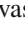
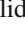




Karlsruher Institut fuer Technologie, Karlsruhe, Germany

S. Brommer , M. Burkart, E. Butz , T. Chwalek , A. Dierlamm , A. Droll, N. Faltermann , M. Giffels , A. Gottmann , F. Hartmann ³¹, R. Hofsaess , M. Horzela , U. Husemann , M. Klute , R. Koppenhöfer , M. Link, A. Lintuluoto , S. Maier , S. Mitra , M. Mormile , Th. Müller , M. Neukum, M. Oh , G. Quast , K. Rabbertz , B. Regnery , N. Shadskiy , I. Shvetsov , H. J. Simonis , N. Trevisani , R. Ulrich , J. van der Linden , R. F. Von Cube , M. Wassmer , S. Wieland , F. Wittig, R. Wolf , S. Wunsch, X. Zuo 


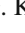


Institute of Nuclear and Particle Physics (INPP), NCSR Demokritos, Agia Paraskevi, Greece

G. Anagnostou, P. Assiouras , G. Daskalakis , A. Kyriakis, A. Papadopoulos³¹, A. Stakia 






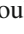

National and Kapodistrian University of Athens, Athens, Greece

P. Kontaxakis , G. Melachroinos, A. Panagiotou, I. Papavergou , I. Paraskevas , N. Saoulidou , K. Theofilatos , E. Tziaferi , K. Vellidis , I. Zisopoulos 

National Technical University of Athens, Athens, Greece

G. Bakas , T. Chatzistavrou, G. Karapostoli , K. Kousouris , I. Papakrivopoulos , E. Siamarkou, G. Tsiopolitis, A. Zacharopoulou

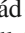


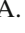

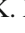



University of Ioánnina, Ioannina, Greece

K. Adamidis, I. Bestintzanos, I. Evangelou , C. Foudas, P. Gianneios , C. Kamtsikis, P. Katsoulis, P. Kokkas , P. G. Kosmoglou Kioseoglou , N. Manthos , I. Papadopoulos , J. Strologas 

HUN-REN Wigner Research Centre for Physics, Budapest, Hungary

M. Bartók ³², C. Hajdu , D. Horvath ^{33,34}, F. Sikler , V. Veszpremi 

MTA-ELTE Lendület CMS Particle and Nuclear Physics Group, Eötvös Loránd University, Budapest, Hungary

M. Csanád , K. Farkas , M. M. A. Gadallah ³⁵, Á. Kadlecik , P. Major , K. Mandal , G. Pásztor , A. J. Rádl ³⁶, G. I. Veres 

Faculty of Informatics, University of Debrecen, Debrecen, Hungary

P. Raics, B. Ujvari ³⁷, G. Zilizi 




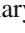
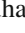









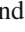
Institute of Nuclear Research ATOMKI, Debrecen, Hungary

G. Bencze, S. Czellar, J. Karancsi ³², J. Molnar, Z. Szillasi

MATE Institute of Technology, Karoly Robert Campus, Gyongyos, Hungary

T. Csorgo ³⁶, F. Nemes ³⁶, T. Novak 







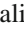


Panjab University, Chandigarh, India

J. Babbar , S. Bansal , S. B. Beri, V. Bhatnagar , G. Chaudhary , S. Chauhan , N. Dhingra ³⁸, R. Gupta, A. Kaur , A. Kaur , H. Kaur , M. Kaur , S. Kumar , M. Meena , K. Sandeep , T. Sheokand, J. B. Singh , A. Singla 

University of Delhi, Delhi, India

A. Ahmed , A. Bhardwaj , A. Chhetri , B. C. Choudhary , A. Kumar , M. Naimuddin , K. Ranjan , S. Saumya 

Saha Institute of Nuclear Physics, HBNI, Kolkata, India

S. Acharya ³⁹, S. Baradia , S. Barman ⁴⁰, S. Bhattacharya , D. Bhowmik, S. Dutta , S. Dutta, B. Gomber ³⁹, P. Palit , G. Saha , B. Sahu ³⁹, S. Sarkar

Indian Institute of Technology Madras, Chennai, India

M. M. Ameen , P. K. Behera , S. C. Behera , S. Chatterjee , P. Jana , P. Kalbhor , J. R. Komaragiri ⁴¹, D. Kumar ⁴¹, L. Panwar ⁴¹, R. Pradhan , P. R. Pujahari , N. R. Saha , A. Sharma , A. K. Sikdar , S. Verma 

Tata Institute of Fundamental Research-A, Mumbai, India

T. Aziz, I. Das , S. Dugad, M. Kumar , G. B. Mohanty , P. Suryadevara

Tata Institute of Fundamental Research-B, Mumbai, India

A. Bala , S. Banerjee , R. M. Chatterjee, M. Guchait , Sh. Jain , S. Karmakar , S. Kumar , G. Majumder , K. Mazumdar , S. Mukherjee , A. Thachayath 

National Institute of Science Education and Research, An OCC of Homi Bhabha National Institute, Bhubaneswar, Odisha, India

S. Bahinipati ⁴², A. K. Das, C. Kar , D. Maity ⁴³, P. Mal , T. Mishra , V. K. Muraleedharan Nair Bindhu ⁴³, K. Naskar ⁴³, A. Nayak ⁴³, P. Sadangi, P. Saha , S. K. Swain , S. Varghese ⁴³, D. Vats ⁴³

Indian Institute of Science Education and Research (IISER), Pune, India

A. Alpana , S. Dube , B. Kansal , A. Laha , A. Rastogi , S. Sharma 


Isfahan University of Technology, Isfahan, Iran

H. Bakhshiansohi ⁴⁴, E. Khazaie ⁴⁴, M. Zeinali ⁴⁵








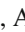




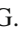




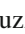







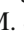




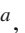
Institute for Research in Fundamental Sciences (IPM), Tehran, Iran

S. Chenarani ⁴⁶, S. M. Etesami , M. Khakzad , M. Mohammadi Najafabadi 




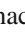








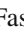













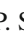
University College Dublin, Dublin, Ireland

M. Grunewald 

INFN Sezione di Bari^a, Università di Bari^b, Politecnico di Bari^c, Bari, Italy

M. Abbrescia ^{a,b}, R. Aly ^{a,c,47}, A. Colaleo ^{a,b}, D. Creanza ^{a,c}, B. D'Anzi ^{a,b}, N. De Filippis ^{a,c}, M. De Palma ^{a,b}, A. Di Florio ^{a,c}, W. Elmetenawee ^{a,b,47}, L. Fiore ^a, G. Iaselli ^{a,c}, G. Maggi ^{a,c}, M. Maggi ^a, I. Margjeka ^{a,b}, V. Mastrapasqua ^{a,b}, S. My ^{a,b}, S. Nuzzo ^{a,b}, A. Pellicchia ^{a,b}, A. Pompili ^{a,b}, G. Pugliese ^{a,c}, R. Radogna ^a, G. Ramirez-Sanchez ^{a,c}, D. Ramos ^a, A. Ranieri ^a, L. Silvestris ^a, F. M. Simone ^{a,b}, Ü. Sözbilir ^a, A. Stamerra ^a, R. Venditti ^a, P. Verwilligen ^a, A. Zaza ^{a,b}



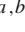
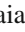
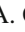








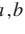


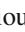
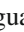
INFN Sezione di Bologna^a, Università di Bologna^b, Bologna, Italy

G. Abbiendi ^a, C. Battilana ^{a,b}, D. Bonacorsi ^{a,b}, L. Borgonovi ^a, R. Campanini ^{a,b}, P. Capiluppi ^{a,b}, A. Castro ^{a,b}, F. R. Cavallo ^a, M. Cuffiani ^{a,b}, G. M. Dallavalle ^a, T. Diotallevi ^{a,b}, A. Fanfani ^{a,b}, D. Fasanella ^{a,b}, P. Giacomelli ^a, L. Giommi ^{a,b}, C. Grandi ^a, L. Guiducci ^{a,b}, S. Lo Meo ^{a,48}, L. Lunerti ^{a,b}, S. Marcellini ^a, G. Masetti ^a, F. L. Navarria ^{a,b}, A. Perrotta ^a, F. Primavera ^{a,b}, A. M. Rossi ^{a,b}, T. Rovelli ^{a,b}, G. P. Siroli ^{a,b}

INFN Sezione di Catania^a, Università di Catania^b, Catania, Italy

S. Costa ^{a,b,49}, A. Di Mattia ^a, R. Potenza ^{a,b}, A. Tricomi ^{a,b,49}, C. Tuve ^{a,b}





INFN Sezione di Firenze^a, Università di Firenze^b, Florence, Italy

G. Barbagli ^a, G. Bardelli ^{a,b}, B. Camaiani ^{a,b}, A. Cassese ^a, R. Ceccarelli ^a, V. Ciulli ^{a,b}, C. Civinini ^a, R. D'Alessandro ^{a,b}, E. Focardi ^{a,b}, T. Kello ^a, G. Latino ^{a,b}, P. Lenzi ^{a,b}, M. Lizzo ^a, M. Meschini ^a, S. Paoletti ^a, A. Papanastassiou ^{a,b}, G. Sguazzoni ^a, L. Viliani ^a



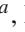







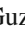
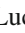

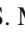



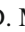






INFN Laboratori Nazionali di Frascati, Frascati, Italy

L. Benussi , S. Bianco , S. Meola ⁵⁰, D. Piccolo 




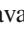

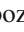


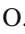

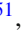
INFN Sezione di Genova^a, Università di Genova^b, Genoa, Italy

P. Chatagnon ^a, F. Ferro ^a, E. Robutti ^a, S. Tosi ^{a,b}



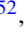

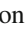








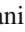
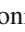








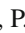
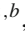





INFN Sezione di Milano-Bicocca^a, Università di Milano-Bicocca^b, Milan, Italy

A. Benaglia , G. Boldrini , F. Brivio , F. Cetorelli , F. De Guio , M. E. Dinardo , P. Dini , S. Gennai , A. Ghezzi , P. Govoni , L. Guzzi , M. T. Lucchini , M. Malberti , S. Malvezzi , A. Massironi , D. Menasce , L. Moroni , M. Paganoni , D. Pedrini , B. S. Pinolini , S. Ragazzi , N. Redaelli , T. Tabarelli de Fatis , D. Zuolo 

INFN Sezione di Napoli^a, Università di Napoli ‘Federico II’^b, Naples, Italy; Università della Basilicata^c, Potenza, Italy; Scuola Superiore Meridionale (SSM)^d, Naples, Italy

S. Buontempo , A. Cagnotta , F. Carnevali , N. Cavallo , A. De Iorio , F. Fabozzi , A. O. M. Iorio , L. Lista , P. Paolucci , B. Rossi , C. Sciacca 

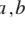
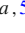

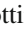

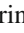





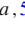




INFN Sezione di Padova^a, Università di Padova^b, Padua, Italy; Università di Trento^c, Trento, Italy

R. Ardino , P. Azzi , N. Bacchetta , D. Bisello , P. Bortignon , A. Bragagnolo , R. Carlin , P. Checchia , T. Dorigo , U. Gasparini , G. Grosso , L. Layer , E. Lusiani , M. Margoni , A. T. Meneguzzo , M. Michelotto , M. Migliorini , F. Montecassiano , J. Pazzini , P. Ronchese , R. Rossin , F. Simonetto , G. Strong , M. Tosi , A. Triossi , S. Ventura , H. Yarar , P. Zotto , A. Zucchetta , G. Zumerle 



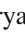








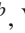

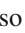







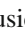


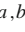






INFN Sezione di Pavia^a, Università di Pavia^b, Pavia, Italy

S. Abu Zeid , C. Aimè , A. Braghieri , S. Calzaferrì , D. Fiorina , P. Montagna , V. Re , C. Riccardi , P. Salvini , I. Vai , P. Vitulo 

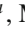


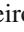
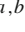

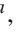







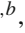
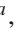



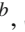
INFN Sezione di Perugia^a, Università di Perugia^b, Perugia, Italy

S. Ajmal , P. Asenov , G. M. Bilei , D. Ciangottini , L. Fanò , M. Magherini , G. Mantovani , V. Mariani , M. Menichelli , F. Moscatelli , A. Piccinelli , M. Presilla , A. Rossi , A. Santocchia , D. Spiga , T. Tedeschi 


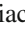










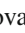







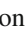


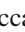



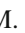











INFN Sezione di Pisa^a, Università di Pisa^b, Scuola Normale Superiore di Pisa^c, Pisa, Italy; Università di Siena^d, Siena, Italy

P. Azzurri , G. Bagliesi , R. Bhattacharya , L. Bianchini , T. Boccali , E. Bossini , D. Bruschini , R. Castaldi , M. A. Ciocci , M. Cipriani , V. D’Amante , R. Dell’Orso , S. Donato , A. Giassi , F. Ligabue , D. Matos Figueiredo , A. Messineo , M. Musich , F. Palla , S. Parolia , A. Rizzi , G. Rolandi , S. Roy Chowdhury , T. Sarkar , A. Scribano , P. Spagnolo , R. Tenchini , G. Tonelli , N. Turini , A. Venturi , P. G. Verdini 






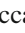
INFN Sezione di Roma^a, Sapienza Università di Roma^b, Rome, Italy

P. Barria , M. Campana , F. Cavallari , L. Cunqueiro Mendez , D. Del Re , E. Di Marco , M. Diemmoz , F. Errico , E. Longo , P. Meridiani , J. Mijuskovic , G. Organtini , F. Pandolfi , R. Paramatti , C. Quaranta , S. Rahatlou , C. Rovelli , F. Santanastasio , L. Soffi , R. Tramontano 

INFN Sezione di Torino^a, Università di Torino^b, Turin, Italy; Università del Piemonte Orientale^c, Novara, Italy

N. Amapane , R. Arcidiacono , S. Argiro , M. Arneodo , N. Bartosik , R. Bellan , A. Bellora , C. Biino , N. Cartiglia , M. Costa , R. Covarelli , N. Demaria , L. Finco , M. Grippo , B. Kiani , F. Legger , F. Luongo , C. Mariotti , S. Maselli , A. Mecca , E. Migliore , M. Monteno , R. Mulargia , M. M. Obertino , G. Ortona , L. Pacher , N. Pastrone , M. Pelliccioni , M. Ruspà , F. Siviero , V. Sola , A. Solano , D. Soldi , A. Staiano , C. Tarricone , M. Tornago , D. Trocino , G. Umoret , E. Vlasov 

INFN Sezione di Trieste^a, Università di Trieste^b, Trieste, Italy

S. Belforte , V. Candelise , M. Casarsa , F. Cossutti , K. De Leo , G. Della Ricca 

Kyungpook National University, Daegu, Korea

S. Dogra , J. Hong , C. Huh , B. Kim , D. H. Kim , J. Kim , H. Lee , S. W. Lee , C. S. Moon , Y. D. Oh , M. S. Ryu , S. Sekmen , Y. C. Yang 


Institute for Universe and Elementary Particles, Chonnam National University, Kwangju, Korea

G. Bak , P. Gwak , H. Kim , D. H. Moon 

Hanyang University, Seoul, Korea

E. Asilar , D. Kim , T. J. Kim , J. A. Merlin, J. Park 

Korea University, Seoul, Korea

S. Choi , S. Han, B. Hong , K. Lee, K. S. Lee , S. Lee , J. Park, S. K. Park, J. Yoo 

Department of Physics, Kyung Hee University, Seoul, Korea

J. Goh 


Sejong University, Seoul, Korea

H. S. Kim , Y. Kim, S. Lee

Seoul National University, Seoul, Korea

J. Almond, J. H. Bhyun, J. Choi , W. Jun , J. Kim , J. S. Kim, S. Ko , H. Kwon , H. Lee , J. Lee , J. Lee , B. H. Oh , S. B. Oh , H. Seo , U. K. Yang, I. Yoon 

University of Seoul, Seoul, Korea

W. Jang , D. Y. Kang, Y. Kang , S. Kim , B. Ko, J. S. H. Lee , Y. Lee , I. C. Park , Y. Roh, I. J. Watson , S. Yang 


Department of Physics, Yonsei University, Seoul, Korea

S. Ha , H. D. Yoo 

Sungkyunkwan University, Suwon, Korea

M. Choi , M. R. Kim , H. Lee, Y. Lee , I. Yu 


College of Engineering and Technology, American University of the Middle East (AUM), Dasman, Kuwait

T. Beyrouthy, Y. Maghrbi 

Riga Technical University, Riga, Latvia

K. Dreimanis , A. Gaile , G. Pikurs, A. Potrebko , M. Seidel , V. Veckalns  ⁵⁶

University of Latvia (LU), Riga, Latvia

N. R. Strautnieks 

Vilnius University, Vilnius, Lithuania

M. Ambrozias , A. Juodagalvis , A. Rinkevicius , G. Tamulaitis 

National Centre for Particle Physics, Universiti Malaya, Kuala Lumpur, Malaysia

N. Bin Norjoharuddeen , I. Yusuff  ⁵⁷, Z. Zolkapli

Universidad de Sonora (UNISON), Hermosillo, Mexico

J. F. Benitez , A. Castaneda Hernandez , H. A. Encinas Acosta, L. G. Gallegos Maríñez, M. León Coello , J. A. Murillo Quijada , A. Sehrawat , L. Valencia Palomo 

Centro de Investigacion y de Estudios Avanzados del IPN, Mexico City, Mexico

G. Ayala , H. Castilla-Valdez , E. De La Cruz-Burelo , I. Heredia-De La Cruz  ⁵⁸, R. Lopez-Fernandez , C. A. Mondragon Herrera, A. Sánchez Hernández 

Universidad Iberoamericana, Mexico City, Mexico

C. Oropeza Barrera , M. Ramírez García 

Benemerita Universidad Autonoma de Puebla, Puebla, Mexico

I. Bautista , I. Pedraza , H. A. Salazar Ibarguen , C. Uribe Estrada 


University of Montenegro, Podgorica, Montenegro

I. Bubanja, N. Raicevic 

University of Canterbury, Christchurch, New Zealand

P. H. Butler 

National Centre for Physics, Quaid-I-Azam University, Islamabad, Pakistan

A. Ahmad , M. I. Asghar, A. Awais , M. I. M. Awan, H. R. Hoorani , W. A. Khan 

Faculty of Computer Science, Electronics and Telecommunications, AGH University of Krakow, Kraków, Poland

V. Avati, L. Grzanka , M. Malawski 



National Centre for Nuclear Research, Swierk, Poland

H. Bialkowska , M. Bluj , B. Boimska , M. Górski , M. Kazana , M. Szeper , P. Zalewski 

Institute of Experimental Physics, Faculty of Physics, University of Warsaw, Warsaw, Poland

K. Bunkowski , K. Doroba , A. Kalinowski , M. Konecki , J. Krolikowski , A. Muhammad 



Warsaw University of Technology, Warsaw, Poland

K. Pozniak , W. Zabolotny 

Laboratório de Instrumentação e Física Experimental de Partículas, Lisbon, Portugal

M. Araujo , D. Bastos , C. Beirão Da Cruz E Silva , A. Boletti , M. Bozzo , P. Faccioli , M. Gallinaro , J. Hollar , N. Leonardo , T. Niknejad , A. Petrilli , M. Pisano , J. Seixas , J. Varela , J. W. Wulff






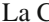











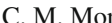

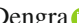







Faculty of Physics, University of Belgrade, Belgrade, Serbia

P. Adzic , P. Milenovic 

VINCA Institute of Nuclear Sciences, University of Belgrade, Belgrade, Serbia

M. Dordevic , J. Milosevic , V. Rekovic









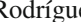




Centro de Investigaciones Energéticas Medioambientales y Tecnológicas (CIEMAT), Madrid, Spain

M. Aguilar-Benitez, J. Alcaraz Maestre , Cristina F. Bedoya , M. Cepeda , M. Cerrada , N. Colino , B. De La Cruz , A. Delgado Peris , D. Fernández Del Val , J. P. Fernández Ramos , J. Flix , M. C. Fouz , O. Gonzalez Lopez , S. Goy Lopez , J. M. Hernandez , M. I. Josa , J. León Holgado , D. Moran , C. M. Morcillo Perez , Á. Navarro Tobar , C. Perez Dengra , A. Pérez-Calero Yzquierdo , J. Puerta Pelayo , I. Redondo , D. D. Redondo Ferrero , L. Romero, S. Sánchez Navas , L. Urda Gómez , J. Vazquez Escobar , C. Willmott






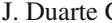













Universidad Autónoma de Madrid, Madrid, Spain

J. F. de Trocóniz 

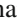
Instituto Universitario de Ciencias y Tecnologías Espaciales de Asturias (ICTEA), Universidad de Oviedo, Oviedo, Spain

B. Alvarez Gonzalez , J. Cuevas , J. Fernandez Menendez , S. Folgueras , I. Gonzalez Caballero , J. R. González Fernández , E. Palencia Cortezon , C. Ramón Álvarez , V. Rodríguez Bouza , A. Soto Rodríguez , A. Trapote , C. Vico Villalba , P. Vischia 





Instituto de Física de Cantabria (IFCA), CSIC-Universidad de Cantabria, Santander, Spain

S. Bhowmik , S. Blanco Fernández , J. A. Brochero Cifuentes , I. J. Cabrillo , A. Calderon , J. Duarte Campderros , M. Fernandez , C. Fernandez Madrazo , G. Gomez , C. Lasaos García , C. Martinez Rivero , P. Martinez Ruiz del Arbol , F. Matorras , P. Matorras Cuevas , E. Navarrete Ramos , J. Piedra Gomez , L. Scodellaro , I. Vila , J. M. Vizan Garcia 








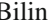
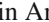


















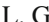





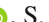


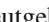







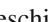
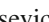
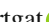



University of Colombo, Colombo, Sri Lanka

























M. K. Jayananda , B. Kailasapathy ⁵⁹, D. U. J. Sonnadara , D. D. C. Wickramarathna 

Department of Physics, University of Ruhuna, Matara, Sri Lanka










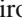


W. G. D. Dharmaratna ⁶⁰, K. Liyanage , N. Perera , N. Wickramage 

CERN, European Organization for Nuclear Research, Geneva, Switzerland






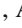









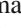
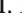



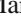
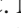


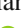


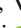


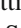
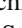



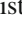

D. Abbaneo , C. Amendola , E. Auffray , G. Auzinger , J. Baechler, D. Barney , A. Bermúdez Martínez , M. Bianco , B. Bilin , A. A. Bin Anuar , A. Bocci , E. Brondolin , C. Caillol , T. Camporesi , G. Cerminara , N. Chernyavskaya , D. d'Enterria , A. Dabrowski , A. David , A. De Roeck , M. M. Defranchis , M. Deile , M. Dobson , F. Fallavollita⁶¹, L. Forthomme , G. Franzoni , W. Funk , S. Giani, D. Gigi, K. Gill , F. Glege , L. Gouskos , M. Haranko , J. Hegeman , V. Innocente , T. James , P. Janot , J. Kieseler , S. Laurila , P. Lecoq , E. Leutgeb , C. Lourenço , B. Maier , L. Malgeri , M. Mannelli , A. C. Marini , F. Meijers , S. Mersi , E. Meschi , V. Milosevic , F. Moortgat , M. Mulders , S. Orfanelli, F. Pantaleo , M. Peruzzi 

G. Petrucciani , A. Pfeiffer , M. Pierini , D. Piparo , H. Qu , D. Raby , G. Reales Gutiérrez, M. Rovere , H. Sakulin , S. Scarfi , M. Selvaggi , A. Sharma , K. Shchelina , P. Silva , P. Sphicas ⁶², A. G. Stahl Leitner , A. Steen , S. Summers , D. Treille , P. Tropea , A. Tsiros, D. Walter , J. Wanczyk ⁶³, K. A. Wozniak ⁶⁴, P. Zehetner , P. Zejdl , W. D. Zeuner




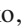






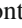
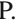



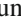
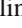





Paul Scherrer Institut, Villigen, Switzerland

T. Bevilacqua ⁶⁵, L. Caminada ⁶⁵, A. Ebrahimi , W. Erdmann , R. Horisberger , Q. Ingram , H. C. Kaestli , D. Kotlinski , C. Lange , M. Missiroli ⁶⁵, L. Noehte ⁶⁵, T. Rohe 



ETH Zurich-Institute for Particle Physics and Astrophysics (IPA), Zurich, Switzerland

T. K. Aarrestad , K. Androsov ⁶³, M. Backhaus , A. Calandri , C. Cazzaniga , K. Datta , A. De Cosa , G. Dissertori , M. Dittmar, M. Donegà , F. Eble , M. Galli , K. Gedia , F. Glessgen , C. Grab , D. Hits , W. Lustermann , A.-M. Lyon , R. A. Manzoni , M. Marchegiani , L. Marchese , C. Martin Perez , A. Mascellani ⁶³, F. Nessi-Tedaldi , F. Pauss , V. Perovic , S. Pigazzini , M. G. Ratti , M. Reichmann , C. Reissel , T. Reitenspiess , B. Ristic , F. Riti , D. Ruini, D. A. Sanz Becerra , R. Seidita , J. Steggemann ⁶³, D. Valsecchi , R. Wallny 


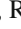
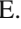
Universität Zürich, Zurich, Switzerland

C. AMSLER ⁶⁶, P. Bäertschi , C. Botta , D. Brzhechko, M. F. Canelli , K. Cormier , R. Del Burgo, J. K. Heikkilä , M. Huwiler , W. Jin , A. Jofrehei , B. Kilminster , S. Leontsinis , S. P. Liechti , A. Macchiolo , P. Meiring , V. M. Mikuni , U. Molinatti , I. Neutelings , A. Reimers , P. Robmann, S. Sanchez Cruz , K. Schweiger , M. Senger , Y. Takahashi 

National Central University, Chung-Li, Taiwan

C. Adloff⁶⁷, C. M. Kuo, W. Lin, P. K. Rout , P. C. Tiwari ⁴¹, S. S. Yu 


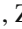


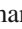


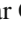


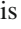
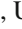


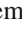


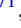

National Taiwan University (NTU), Taipei, Taiwan

L. Ceard, Y. Chao , K. F. Chen , P. S. Chen, Z. G. Chen, W.-S. Hou , T. H. Hsu, Y. W. Kao, R. Khurana, G. Kole , Y. Y. Li , R.-S. Lu , E. Paganis , A. Psallidas, X. F. Su , J. Thomas-Wilsker , H. y. Wu, E. Yazgan 

High Energy Physics Research Unit, Department of Physics, Faculty of Science, Chulalongkorn University, Bangkok, Thailand

C. Asawatangtrakuldee , N. Srimanobhas , V. Wachirapusanand 

Physics Department, Science and Art Faculty, Çukurova University, Adana, Turkey

D. Agyel , F. Boran , Z. S. Demiroglu , F. Dolek , I. Dumanoglu ⁶⁸, E. Eskut , Y. Guler ⁶⁹, E. Gurpinar Guler ⁶⁹, C. Isik , O. Kara, A. Kayis Topaksu , U. Kiminsu , G. Onengut , K. Ozdemir ⁷⁰, A. Polatoz , B. Tali ⁷¹, U. G. Tok , S. Turkcapar , E. Uslan , I. S. Zorbakir 

Physics Department, Middle East Technical University, Ankara, Turkey

M. Yalvac ⁷²








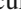
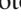
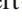

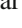

Bogazici University, Istanbul, Turkey

B. Akgun , I. O. Atakisi , E. Gülmez , M. Kaya ⁷³, O. Kaya ⁷⁴, S. Tekten ⁷⁵

Istanbul Technical University, Istanbul, Turkey

A. Cakir , K. Cankocak ⁶⁸, Y. Komurcu , S. Sen ⁷⁶

Istanbul University, Istanbul, Turkey

O. Aydılek , S. Cerci ⁷¹, V. Epshteyn , B. Hacisahinoglu , I. Hos ⁷⁷, B. Isildak ⁷⁸, B. Kaynak , S. Ozkorucuklu , O. Potok , H. Sert , C. Simsek , D. Sunar Cerci ⁷¹, C. Zorbilmez 

Institute for Scintillation Materials of National Academy of Science of Ukraine, Kharkiv, Ukraine









A. Boyaryntsev , B. Grynyov 

National Science Centre, Kharkiv Institute of Physics and Technology, Kharkiv, Ukraine












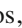

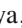

L. Levchuk 

University of Bristol, Bristol, UK





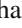









D. Anthony , J. J. Brooke , A. Bundock , F. Bury , E. Clement , D. Cussans , H. Flacher , M. Glowacki,

J. Goldstein , H. F. Heath , L. Kreczko , B. Krikler , S. Paramesvaran , S. Seif El Nasr-Storey, V. J. Smith , N. Stylianou ⁷⁹, K. Walkingshaw Pass, R. White 




Rutherford Appleton Laboratory, Didcot, UK

A. H. Ball, K. W. Bell , A. Belyaev ⁸⁰, C. Brew , R. M. Brown , D. J. A. Cockerill , C. Cooke , K. V. Ellis, K. Harder , S. Harper , M.-L. Holmberg ⁸¹, J. Linacre , K. Manolopoulos, D. M. Newbold , E. Olaiya, D. Petyt , T. Reis , G. Salvi , T. Schuh, C. H. Shepherd-Themistocleous , I. R. Tomalin , T. Williams

Imperial College, London, UK

R. Bainbridge , P. Bloch , C. E. Brown , O. Buchmuller, V. Cacchio, C. A. Carrillo Montoya , G. S. Chahal ⁸², D. Colling , J. S. Dancu, P. Dauncey , G. Davies , J. Davies, M. Della Negra , S. Fayer, G. Fedi , G. Hall , M. H. Hassanshahi , A. Howard, G. Iles , M. Knight , J. Langford , L. Lyons , A.-M. Magnan , S. Malik, A. Martelli , M. Mieskolainen , J. Nash ⁸³, M. Pesaresi , B. C. Radburn-Smith , A. Richards, A. Rose , C. Seez , R. Shukla , A. Tapper , K. Uchida , G. P. Uttley , L. H. Vage, T. Virdee ³¹, M. Vojinovic , N. Wardle , D. Winterbottom

Brunel University, Uxbridge, UK

K. Coldham, J. E. Cole , A. Khan, P. Kyberd , I. D. Reid 

Baylor University, Waco, TX, USA

S. Abdullin , A. Brinkerhoff , B. Caraway , J. Dittmann , K. Hatakeyama , J. Hiltbrand , A. R. Kanuganti , B. McMaster , M. Saunders , S. Sawant , C. Sutantawibul , M. Toms ⁸⁴, J. Wilson

Catholic University of America, Washington, DC, USA

R. Bartek , A. Dominguez , C. Huerta Escamilla, A. E. Simsek , R. Uniyal , A. M. Vargas Hernandez 



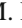

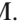




The University of Alabama, Tuscaloosa, AL, USA

R. Chudasama , S. I. Cooper , S. V. Gleyzer , C. U. Perez , P. Rumerio ⁸⁵, E. Usai , C. West , R. Yi 






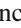



Boston University, Boston, MA, USA

A. Akpinar , A. Albert , D. Arcaro , C. Cosby , Z. Demiragli , C. Erice , E. Fontanesi , D. Gastler , S. Jeon , J. Rohlf , K. Salyer , D. Sperka , D. Spitzbart , I. Suarez , A. Tsatsos , S. Yuan



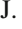


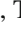



Brown University, Providence, RI, USA

G. Benelli , X. Coubez ²⁶, D. Cutts , M. Hadley , U. Heintz , J. M. Hogan ⁸⁶, T. Kwon , G. Landsberg , K. T. Lau , D. Li , J. Luo , S. Mondal , M. Narain [†], N. Pervan , S. Sagir ⁸⁷, F. Simpson , M. Stamenkovic , W. Y. Wong, X. Yan , W. Zhang





University of California, Davis, Davis, CA, USA

S. Abbott , J. Bonilla , C. Brainerd , R. Breedon , M. Calderon De La Barca Sanchez , M. Chertok , M. Citron , J. Conway , P. T. Cox , R. Erbacher , F. Jensen , O. Kukral , G. Mocellin , M. Mulhearn , D. Pellett , W. Wei , Y. Yao , F. Zhang










University of California, Los Angeles, CA, USA

M. Bachtis , R. Cousins , A. Datta , J. Hauser , M. Ignatenko , M. A. Iqbal , T. Lam , E. Manca , W. A. Nash , D. Saltzberg , B. Stone , V. Valuev






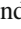



University of California, Riverside, Riverside, CA, USA

R. Clare , M. Gordon, G. Hanson , W. Si , S. Wimpenny [†]

University of California, San Diego, La Jolla, CA, USA

J. G. Branson , S. Cittolin , S. Cooperstein , D. Diaz , J. Duarte , R. Gerosa , L. Giannini , J. Guiang , R. Kansal , V. Krutelyov , R. Lee , J. Letts , M. Masciovecchio , F. Mokhtar , M. Pieri , M. Quinnan , B. V. Sathia Narayanan , V. Sharma , M. Tadel , E. Vourliotis , F. Würthwein , Y. Xiang , A. Yagil

Department of Physics, University of California, Santa Barbara, Santa Barbara, CA, USA

A. Barzdukas , L. Brennan , C. Campagnari , G. Collura , A. Dorsett , J. Incandela , M. Kilpatrick , J. Kim , A. J. Li , P. Masterson , H. Mei , M. Oshiro , J. Richman , U. Sarica , R. Schmitz , F. Setti , J. Sheplock , D. Stuart , S. Wang

Kansas State University, Manhattan, KS, USA

B. Allmond , A. Ivanov , K. Kaadze , A. Kalogeropoulos , D. Kim, Y. Maravin , K. Nam, J. Natoli , D. Roy , G. Sorrentino 



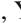

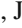







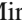





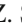





Lawrence Livermore National Laboratory, Livermore, CA, USA

F. Rebassoo , D. Wright 

University of Maryland, College Park, MD, USA

E. Adams , A. Baden , O. Baron, A. Belloni , A. Bethani , Y. M. Chen , S. C. Eno , N. J. Hadley , S. Jabeen , R. G. Kellogg , T. Koeth , Y. Lai , S. Lascio , A. C. Mignerey , S. Nabili , C. Palmer , C. Papageorgakis , M. M. Paranjpe, L. Wang , K. Wong 

Massachusetts Institute of Technology, Cambridge, MA, USA

J. Bendavid , W. Busza , I. A. Cali , Y. Chen , M. D'Alfonso , J. Eysermans , C. Freer , G. Gomez-Ceballos , M. Goncharov, P. Harris, D. Hoang, D. Kovalskiy , J. Krupa , L. Lavezzo , Y.-J. Lee , K. Long , C. Mironov , C. Paus , D. Rankin , C. Roland , G. Roland , S. Rothman , Z. Shi , G. S. F. Stephans , J. Wang, Z. Wang , B. Wyslouch , T. J. Yang 

University of Minnesota, Minneapolis, MN, USA

B. Crossman , B. M. Joshi , C. Kapsiak , M. Krohn , D. Mahon , J. Mans , B. Marzocchi , S. Pandey , M. Revering , R. Rusack , R. Saradhy , N. Schroeder , N. Strobbe , M. A. Wadud 



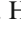
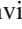





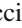

University of Mississippi, Oxford, MS, USA

L. M. Cremaldi 




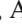
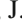


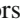





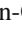
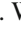

University of Nebraska-Lincoln, Lincoln, NE, USA

K. Bloom , M. Bryson, D. R. Claes , C. Fangmeier , F. Golf , G. Haza , J. Hossain , C. Joo , I. Kravchenko , I. Reed , J. E. Siado , G. R. Snow[†], W. Tabb , A. Vagnerini , A. Wightman , F. Yan , D. Yu , A. G. Zecchinelli 

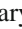
State University of New York at Buffalo, Buffalo, NY, USA

G. Agarwal , H. Bandyopadhyay , L. Hay , I. Iashvili , A. Kharchilava , C. McLean , M. Morris , D. Nguyen , J. Pekkanen , S. Rappoccio , H. Rejeb Sfar, A. Williams 





















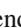



Northeastern University, Boston, MA, USA

G. Alverson , E. Barberis , Y. Haddad , Y. Han , A. Krishna , J. Li , M. Lu , G. Madigan , D. M. Morse , V. Nguyen , T. Orimoto , A. Parker , L. Skinnari , A. Tishelman-Charny , B. Wang , D. Wood 




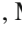


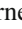


Northwestern University, Evanston, IL, USA

S. Bhattacharya , J. Bueghly, Z. Chen , K. A. Hahn , Y. Liu , Y. Miao , D. G. Monk , M. H. Schmitt , A. Taliercio , M. Velasco

University of Notre Dame, Notre Dame, IN, USA

R. Band , R. Bucci, S. Castells , M. Cremonesi, A. Das , R. Goldouzian , M. Hildreth , K. W. Ho , K. Hurtado Anampa , C. Jessop , K. Lannon , J. Lawrence , N. Loukas , L. Lutton , J. Mariano, N. Marinelli, I. Mcalister, T. McCauley , C. Mcgrady , K. Mohrman , C. Moore , Y. Musienko ¹⁶, H. Nelson , M. Osherson , R. Ruchti , A. Townsend , M. Wayne , H. Yockey, M. Zarucki , L. Zygala 

The Ohio State University, Columbus, OH, USA

A. Basnet , B. Bylsma, M. Carrigan , L. S. Durkin , C. Hill , M. Joyce , A. Lesauvage , M. Nunez Ornelas , K. Wei, B. L. Winer , B. R. Yates 















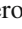


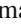
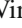


Princeton University, Princeton, NJ, USA

F. M. Addesa , H. Bouchamaoui , P. Das , G. Dezoort , P. Elmer , A. Frankenthal , B. Greenberg , N. Haubrich , S. Higginbotham , G. Kopp , S. Kwan , D. Lange , A. Loeliger , D. Marlow , I. Ojalvo , J. Olsen , D. Stickland , C. Tully 

University of Puerto Rico, Mayagüez, PR, USA

S. Malik 


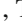









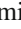
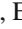

Purdue University, West Lafayette, IN, USA

A. S. Bakshi , V. E. Barnes , S. Chandra , R. Chawla , S. Das , A. Gu , L. Gutay, M. Jones , A. W. Jung , D. Kondratyev , A. M. Koshy, M. Liu , G. Negro , N. Neumeister , G. Paspalaki , S. Piperov , A. Purohit , V. Scheurer, J. F. Schulte , M. Stojanovic , J. Thieman , A. K. Viridi , F. Wang , W. Xie 



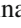


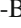
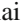


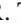

Purdue University Northwest, Hammond, IN, USA

J. Dolen , N. Parashar , A. Pathak 


Rice University, Houston, TX, USA

D. Acosta , A. Baty , T. Carnahan , S. Dildick , K. M. Ecklund , P. J. Fernández Manteca , S. Freed, P. Gardner, F. J. M. Geurts , A. Kumar , W. Li , O. Miguel Colin , B. P. Padley , R. Redjimi, J. Rotter , E. Yigitbasi , Y. Zhang 



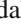



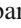


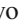


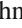


University of Rochester, Rochester, NY, USA

A. Bodek , P. de Barbaro , R. Demina , J. L. Dulemba , C. Fallon, A. Garcia-Bellido , O. Hindrichs , A. Khukhunaishvili , P. Parygin ⁸⁴, E. Popova ⁸⁴, R. Taus , G. P. Van Onsem 

The Rockefeller University, New York, NY, USA

K. Goulianos 

Rutgers, The State University of New Jersey, Piscataway, NJ, USA

B. Chiarito, J. P. Chou , Y. Gershtein , E. Halkiadakis , A. Hart , M. Heindl , D. Jaroslawski , O. Karacheban ²⁹, I. Laflotte , A. Lath , R. Montalvo, K. Nash, H. Routray , S. Salur , S. Schnetzer, S. Somalwar , R. Stone , S. A. Thayil , S. Thomas, J. Vora , H. Wang

University of Tennessee, Knoxville, TN, USA

H. Acharya, D. Ally , A. G. Delannoy , S. Fiorendi , T. Holmes , N. Karunaratna , L. Lee , E. Nibigira , S. Spanier 




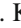





Texas A&M University, College Station, TX, USA

D. Aebi , M. Ahmad , O. Bouhali ⁹⁵, M. Dalchenko , R. Eusebi , J. Gilmore , T. Huang , T. Kamon ⁹⁶, H. Kim , S. Luo , S. Malhotra, R. Mueller , D. Overton , D. Rathjens , A. Safonov 









Texas Tech University, Lubbock, TX, USA

N. Akchurin , J. Damgov , V. Hegde , A. Hussain , Y. Kazhykarim, K. Lamichhane , S. W. Lee , A. Mankel , T. Mengke, S. Muthumuni , T. Peltola , I. Volobouev , A. Whitbeck

Vanderbilt University, Nashville, TN, USA

E. Appelt , S. Greene, A. Gurrola , W. Johns , R. Kunnawalkam Elayavalli , A. Melo , F. Romeo , P. Sheldon , S. Tuo , J. Velkovska , J. Viinikainen

















University of Virginia, Charlottesville, VA, USA

B. Cardwell , B. Cox , J. Hakala , R. Hirosky , A. Ledovskoy , A. Li , C. Neu , C. E. Perez Lara 





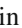







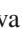




Wayne State University, Detroit, MI, USA





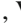





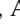

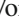


P. E. Karchin 

University of Wisconsin-Madison, Madison, WI, USA

A. Aravind, S. Banerjee , K. Black , T. Bose , S. Dasu , I. De Bruyn , P. Everaerts , C. Galloni, H. He , M. Herndon , A. Herve , C. K. Koraka , A. Lanaro, R. Loveless , J. Madhusudanan Sreekala , A. Mallampalli , A. Mohammadi , S. Mondal, G. Parida , D. Pinna, A. Savin, V. Shang , V. Sharma , W. H. Smith , D. Teague, H. F. Tsoi , W. Vetens , A. Warden

Authors Affiliated with an Institute or an International Laboratory Covered by a Cooperation Agreement with CERN, Geneva, Switzerland

S. Afanasiev , V. Andreev , Yu. Andreev , T. Aushev , M. Azarkin , A. Babaev , A. Belyaev , V. Blinov ⁹⁷, E. Boos , V. Borshch , D. Budkouski , V. Bunichev , M. Chadeeva ⁹⁷, V. Chekhovsky, R. Chistov ⁹⁷, A. Dermenev , T. Dimova ⁹⁷, D. Druzhkin ⁹⁸, M. Dubinin ⁸⁸, L. Dudko , A. Ershov , G. Gavrilo , V. Gavrilo , S. Gninenko , V. Golovtsov , N. Golubev , I. Golutvin , I. Gorbunov , A. Gribushin

Y. Ivanov , V. Kachanov , L. Kardapoltsev ⁹⁷, V. Karjavine , A. Karneyeu , V. Kim ⁹⁷, M. Kirakosyan, D. Kirpichnikov , M. Kirsanov , V. Klyukhin , O. Kodolova ⁹⁹, D. Konstantinov , V. Korenkov , A. Kozyrev ⁹⁷, N. Krasnikov , A. Lanev , P. Levchenko ¹⁰⁰, N. Lychkovskaya , V. Makarenko , A. Malakhov , V. Matveev ⁹⁷, V. Murzin , A. Nikitenko ^{101,99}, S. Obraztsov , V. Oreshkin , V. Palichik , V. Perelygin , M. Perfilov, S. Petrushanko , S. Polikarpov ⁹⁷, V. Popov , O. Radchenko ⁹⁷, M. Savina , V. Savrin , V. Shalaev , S. Shmatov , S. Shulha , Y. Skovpen ⁹⁷, S. Slabospitskii , V. Smirnov , D. Sosnov , V. Sulimov , E. Tcherniaev , A. Terkulov , O. Teryaev , I. Tlisova , A. Toropin , L. Uvarov , A. Uzunian , A. Vorobyev[†], N. Voytishin , B. S. Yuldashev¹⁰², A. Zarubin , I. Zhizhin , A. Zhokin 

† Deceased

- 1: Also at Yerevan State University, Yerevan, Armenia
- 2: Also at TU Wien, Vienna, Austria
- 3: Also at Institute of Basic and Applied Sciences, Faculty of Engineering, Arab Academy for Science, Technology and Maritime Transport, Alexandria, Egypt
- 4: Also at Ghent University, Ghent, Belgium
- 5: Also at Universidade Estadual de Campinas, Campinas, Brazil
- 6: Also at Federal University of Rio Grande do Sul, Porto Alegre, Brazil
- 7: Also at UFMS, Nova Andradina, Brazil
- 8: Also at Nanjing Normal University, Nanjing, China
- 9: Now at Henan Normal University, Xinxiang, China
- 10: Now at The University of Iowa, Iowa City, IA, USA
- 11: Also at University of Chinese Academy of Sciences, Beijing, China
- 12: Also at China Center of Advanced Science and Technology, Beijing, China
- 13: Also at University of Chinese Academy of Sciences, Beijing, China
- 14: Also at China Spallation Neutron Source, Dongguan, Guangdong, China
- 15: Also at Université Libre de Bruxelles, Brussels, Belgium
- 16: Also at an Institute or an International Laboratory Covered by a Cooperation Agreement with CERN, Geneva, Switzerland
- 17: Now at British University in Egypt, Cairo, Egypt
- 18: Now at Cairo University, Cairo, Egypt
- 19: Also at Birla Institute of Technology, Mesra, Mesra, India
- 20: Also at Purdue University, West Lafayette, IN, USA
- 21: Also at Université de Haute Alsace, Mulhouse, France
- 22: Also at Department of Physics, Tsinghua University, Beijing, China
- 23: Also at The University of the State of Amazonas, Manaus, Brazil
- 24: Also at Erzincan Binali Yildirim University, Erzincan, Turkey
- 25: Also at University of Hamburg, Hamburg, Germany
- 26: Also at III. Physikalisches Institut A, RWTH Aachen University, Aachen, Germany
- 27: Also at Isfahan University of Technology, Isfahan, Iran
- 28: Also at Bergische University Wuppertal (BUW), Wuppertal, Germany
- 29: Also at Brandenburg University of Technology, Cottbus, Germany
- 30: Also at Forschungszentrum Jülich, Jülich, Germany
- 31: Also at CERN, European Organization for Nuclear Research, Geneva, Switzerland
- 32: Also at Institute of Physics, University of Debrecen, Debrecen, Hungary
- 33: Also at Institute of Nuclear Research ATOMKI, Debrecen, Hungary
- 34: Now at Universitatea Babeş-Bolyai-Facultatea de Fizica, Cluj-Napoca, Romania
- 35: Also at Physics Department, Faculty of Science, Assiut University, Assiut, Egypt
- 36: Also at HUN-REN Wigner Research Centre for Physics, Budapest, Hungary
- 37: Also at Faculty of Informatics, University of Debrecen, Debrecen, Hungary
- 38: Also at Punjab Agricultural University, Ludhiana, India
- 39: Also at University of Hyderabad, Hyderabad, India
- 40: Also at University of Visva-Bharati, Santiniketan, India
- 41: Also at Indian Institute of Science (IISc), Bangalore, India

- 42: Also at IIT Bhubaneswar, Bhubaneswar, India
- 43: Also at Institute of Physics, Bhubaneswar, India
- 44: Also at Department of Physics, Isfahan University of Technology, Isfahan, Iran
- 45: Also at Sharif University of Technology, Tehran, Iran
- 46: Also at Department of Physics, University of Science and Technology of Mazandaran, Behshahr, Iran
- 47: Also at Helwan University, Cairo, Egypt
- 48: Also at Italian National Agency for New Technologies, Energy and Sustainable Economic Development, Bologna, Italy
- 49: Also at Centro Siciliano di Fisica Nucleare e di Struttura Della Materia, Catania, Italy
- 50: Also at Università degli Studi Guglielmo Marconi, Rome, Italy
- 51: Also at Scuola Superiore Meridionale, Università di Napoli 'Federico II', Naples, Italy
- 52: Also at Fermi National Accelerator Laboratory, Batavia, IL, USA
- 53: Also at Università di Napoli 'Federico II', Naples, Italy
- 54: Also at Ain Shams University, Cairo, Egypt
- 55: Also at Consiglio Nazionale delle Ricerche-Istituto Officina dei Materiali, Perugia, Italy
- 56: Also at Riga Technical University, Riga, Latvia
- 57: Also at Department of Applied Physics, Faculty of Science and Technology, Universiti Kebangsaan Malaysia, Bangi, Malaysia
- 58: Also at Consejo Nacional de Ciencia y Tecnología, Mexico City, Mexico
- 59: Also at Trincomalee Campus, Eastern University, Sri Lanka, Nilaveli, Sri Lanka
- 60: Also at Saegis Campus, Nugegoda, Sri Lanka
- 61: Also at INFN Sezione di Pavia, Università di Pavia, Pavia, Italy
- 62: Also at National and Kapodistrian University of Athens, Athens, Greece
- 63: Also at Ecole Polytechnique Fédérale Lausanne, Lausanne, Switzerland
- 64: Also at University of Vienna Faculty of Computer Science, Vienna, Austria
- 65: Also at Universität Zürich, Zurich, Switzerland
- 66: Also at Stefan Meyer Institute for Subatomic Physics, Vienna, Austria
- 67: Also at Laboratoire d'Annecy-le-Vieux de Physique des Particules, IN2P3-CNRS, Annecy-le-Vieux, France
- 68: Also at Near East University, Research Center of Experimental Health Science, Mersin, Turkey
- 69: Also at Konya Technical University, Konya, Turkey
- 70: Also at Izmir Bakircay University, Izmir, Turkey
- 71: Also at Adiyaman University, Adiyaman, Turkey
- 72: Also at Bozok Universitesi Rektörlüğü, Yozgat, Turkey
- 73: Also at Marmara University, Istanbul, Turkey
- 74: Also at Milli Savunma University, Istanbul, Turkey
- 75: Also at Kafkas University, Kars, Turkey
- 76: Also at Hacettepe University, Ankara, Turkey
- 77: Also at Faculty of Engineering, Istanbul University-Cerrahpasa, Istanbul, Turkey
- 78: Also at Yildiz Technical University, Istanbul, Turkey
- 79: Also at Vrije Universiteit Brussel, Brussels, Belgium
- 80: Also at School of Physics and Astronomy, University of Southampton, Southampton, UK
- 81: Also at University of Bristol, Bristol, UK
- 82: Also at IPPP Durham University, Durham, UK
- 83: Also at Faculty of Science, Monash University, Clayton, Australia
- 84: Now at an Institute or an International Laboratory Covered by a Cooperation Agreement with CERN, Geneva, Switzerland
- 85: Also at Università di Torino, Turin, Italy
- 86: Also at Bethel University, St. Paul, MN, USA
- 87: Also at Karamanoğlu Mehmetbey University, Karaman, Turkey
- 88: Also at California Institute of Technology, Pasadena, CA, USA
- 89: Also at United States Naval Academy, Annapolis, MD, USA
- 90: Also at Bingol University, Bingol, Turkey
- 91: Also at Georgian Technical University, Tbilisi, Georgia
- 92: Also at Sinop University, Sinop, Turkey

-
- 93: Also at Erciyes University, Kayseri, Turkey
94: Also at Horia Hulubei National Institute of Physics and Nuclear Engineering (IFIN-HH), Bucharest, Romania
95: Also at Texas A&M University at Qatar, Doha, Qatar
96: Also at Kyungpook National University, Daegu, Korea
97: Also at Another Institute or International Laboratory Covered by a Cooperation Agreement with CERN, Geneva, Switzerland
98: Also at Universiteit Antwerpen, Antwerp, Belgium
99: Also at Yerevan Physics Institute, Yerevan, Armenia
100: Also at Northeastern University, Boston, MA, USA
101: Also at Imperial College, London, UK
102: Also at Institute of Nuclear Physics of the Uzbekistan Academy of Sciences, Tashkent, Uzbekistan